Thermodynamics of Inter- and Intramolecular Hydrogen Bonding in (Diphosphine)platinum(II) Diolate Complexes and Its Role in Carbohydrate Complexation Regioselectivity

Mark A. Andrews,*,† Gerald K. Cook, and Zachary H. Shriver

Chemistry Department, Brookhaven National Laboratory, P.O. Box 5000, Upton, New York 11973-5000

Received July 9, 1997[⊗]

Thermodynamic data are reported for intermolecular hydrogen-bonding association of 1 and 2 equiv of phenol with [1,3-bis(diphenylphosphino)propane](phenylethane-1,2-diolato)platinum(II) ((dppp)Pt(Ped)) in dichloromethane solution: $\Delta H_1^\circ = -7.0 \pm 0.1$ kcal/mol, $\Delta H_2^\circ = -7.7 \pm 0.4$ kcal/mol, $\Delta S_1^\circ = -11.3 \pm 0.4$ eu, and $\Delta S_2^\circ = -17.8 \pm 1.2$ eu. For comparison, the thermodynamics for hydrogen bonding of phenol to triphenylphosphine oxide in dichloromethane were also determined: $\Delta H^\circ = -5.1 \pm 0.3$ kcal/mol; $\Delta S^\circ = -8.8 \pm 1.0$ eu. Competitive coordination exchange reactions have been used to determine the apparent intramolecular hydrogen bond strengths in (dppp)Pt(1,2-*O*,*O*′-glycerolate) and (dppp)Pt(1,2-*O*,*O*′-butane-1,2,4-triolate) in both dichloromethane ($\Delta G^{313} = -2.05 \pm 0.05$ and -2.52 ± 0.06 kcal/mol, respectively) and pyridine ($\Delta G^{313} = -0.62 \pm 0.03$ and -0.82 ± 0.03 kcal/mol, respectively). Based on these findings, the role of hydrogen-bonding interactions in determining the regioselectivities of complexation of carbohydrates to diphosphine Pt(II) is discussed.

Introduction

We have recently shown that good regioselectivity, a key issue in carbohydrate chemistry, can be achieved in the complexation of sugar alcohols to the metal fragment (diphosphine)platinum(II), e.g., 92% selectivity for formation of (dppp)-Pt(3,4-mannitolate) (Figure 1, dppp = 1,3-bis(diphenylphosphino)-propane).[1] Spectroscopic and structural studies[1−3] implicate strong, multiple *intramolecular* hydrogen bonds as significant contributors to these selectivities. To better evaluate the role of hydrogen bonding in determining carbohydrate complexation regioselectivities, we have undertaken a detailed study of the thermodynamics of both inter- and intramolecular hydrogen bonding in model (diphosphine)platinum(II) diolate complexes. In particular, we wished to compare the strengths of these hydrogen-bonding interactions with other regioselectivity-determining factors and to explore whether intramolecular hydrogen bonding in Pt(II) carbohydrate complexes could compete with intermolecular hydrogen bonding of the carbohydrate hydroxyls to solvents such as pyridine.

The studies reported here offer significant improvements over most prior investigations of intermolecular alcohol−metal alkoxide hydrogen bonding,[4] including more definitive data analyses and determination of both first and second hydrogen-bonding association constants. Furthermore, the ability of these Pt(II) diolate complexes to undergo facile diol−diolate exchange has allowed us to implement a novel approach to the normally difficult problem of quantifying the strength of intramolecular hydrogen bonds. Information on these interactions will assist in the development of metal-catalyzed reactions of carbohydrates that can effect regiospecific syntheses of carbohydrate derivatives or the production of oxygenated organics.[5]

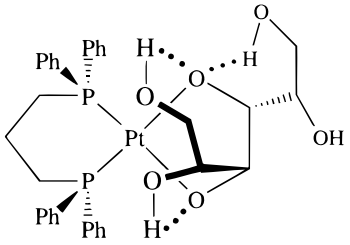

Figure 1. Schematic of X-ray structure of (dppp)Pt(3,4-mannitolate).[1]

Results and Discussion

Background. The interactions of simple metal ions and their inorganic coordination complexes with carbohydrate substrates have been extensively explored.[6−8] Recent X-ray structural and NMR spectroscopic studies conducted by the Klüfers[9] and Chapelle et al.[10] groups, respectively, are particularly definitive with respect to the regioselectivities involved. Such classical coordination complexes can effect a limited range of carbohydrate transformations, one of the most striking being aldose epimerization, which actually involves interchange of C1 and C2.[11,12] Our study of the complexation of alditols to (dppp)-Pt^{II} [1] has begun to extend these inquiries to organotransition metal complexes, the types of metal centers known to serve as

† Current address: The DuPont Co., Experimental Station E328/320, P.O. Box 80328, Wilmington, DE 19880-0328.

⊗ Abstract published in *Advance ACS Abstracts,* November 1, 1997.

(1) Andrews, M. A.; Voss, E. J.; Gould, G. L.; Klooster, W. T.; Koetzle, T. F. *J. Am. Chem. Soc.* **1994**, *116*, 5730−5740.
(2) Appelt, A.; Willis, A. C.; Wild, S. B. *J. Chem. Soc., Chem. Commun.* **1988**, 938−940.
(3) Klooster, W. T.; Voss, E. J.; Andrews, M. A.; Koetzle, T. F. *Abstracts of Papers*, 207th National Meeting of the American Chemical Society, San Diego, CA, March 13−17, 1994; American Chemical Society: Washington, DC, 1994; INOR 292.
(4) For a recent comprehensive summary, see: Kapteijn, G. M.; Dervisi, A.; Grove, D. M.; Kooijman, H.; Lakin, M. T.; Spek, A. L.; van Koten, G. *J. Am. Chem. Soc.* **1995**, *117*, 10939−10949 and references therein.
(5) Cook, G. K.; Andrews, M. A. *J. Am. Chem. Soc.* **1996**, *118*, 9448−9449.
(6) Whitfield, D. M.; Stojkovski, S.; Sarkar, B. *Coord. Chem. Rev.* **1993**, *122*, 171−225.
(7) Angyal, S. J. *Adv. Carbohydr. Chem. Biochem.* **1989**, *47*, 1−43.
(8) Yano, S. *Coord. Chem. Rev.* **1988**, *92*, 113−156.
(9) Burger, J.; Klüfers, P. *Chem. Ber.* **1995**, *128*, 75−79 and references therein.
(10) Chapelle, S.; Sauvage, J. P.; Verchere, J. F. *Inorg. Chem.* **1994**, *33*, 1966−1971 and references therein.
(11) Bilik, V. S., L. *Chem. Zvesti* **1973**, *27*, 544−546.
(12) Hayes, M. L.; Pennings, N. J.; Serianni, A. S.; Barker, R. *J. Am. Chem. Soc.* **1982**, *104*, 6764−6769 and references therein.

S0020-1669(97)00860-4 CCC: $14.00

effective homogeneous catalysts for a much broader range of organic transformations.[13] This is illustrated by our recent report of the deoxydehydration of diols and polyols to alkenes catalyzed by $(C_5Me_5)ReO_3$.[5]

While good regioselective complexation was observed in the Pt alditol system, understanding the origin of these regioselectivities is complicated by the multitude of contributing factors. These include not only axial vs equatorial substitution on the dioxaplatinacyclopentane, as manifested in *threo* vs *erythro* diol complexation preferences, but also strong intramolecular hydrogen bonds between "spectator" hydroxyl groups and the platinum diolate oxygens. These hydrogen-bonding interactions can take the form of five-, six-, or seven-membered rings, all sometimes observed within the same complex as seen in (dppp)-Pt(3,4-mannitolate) (Figure 1). The present studies were designed to explore some of these factors in more detail. The strategy chosen was to first quantify the inherent hydrogen bond acceptor strength of a typical Pt(II) diolate complex and to calibrate against other common hydrogen-bonding systems. This has been accomplished by conducting temperature-dependent equilibrium constant determinations for intermolecular hydrogen bonding of phenol with triphenylphosphine oxide and (dppp)-Pt(phenylethane-1,2-diolate) ((dppp)Pt(Ped)) (eqs 1−3). The

$$Ph_3P{=}O + PhOH \underset{}{\overset{K_{HB}}{\rightleftharpoons}} Ph_3P{=}O \bullet\bullet\bullet\bullet HOPh \qquad (1)$$

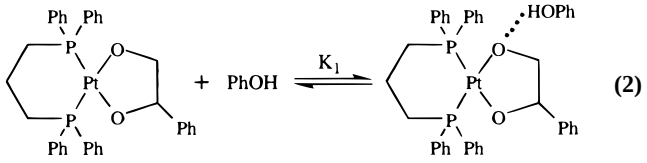

(2)

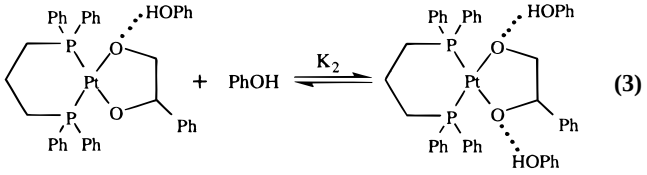

(3)

second step utilized diol−diolate equilibrium exchange reactions with diols containing a pendant "spectator" hydroxyl group at different distances from the diol unit to examine intramolecular hydrogen bond strengths as a function of both hydrogen bond ring size and solvent (eqs 4 and 5).

Intermolecular Hydrogen Bonding. (a) Experimental Design. Hydrogen-bonding studies of organic systems have typically utilized the "noninteracting" solvent carbon tetrachloride.[14,15] Dichloromethane was chosen for the present studies since it provided necessary solubility characteristics for the platinum hydrogen bond acceptor (HBA) complexes, while still having minimal competitive hydrogen bond donor/acceptor properties of its own.[16] Phenol was chosen as the hydrogen bond donor (HBD) since it is a common literature benchmark for ranking hydrogen bond acceptors. While it is known to undergo complicating self-association,[17] this can be eliminated, even in nonpolar media, by working at phenol concentrations

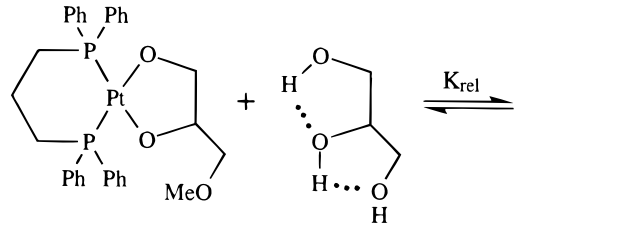

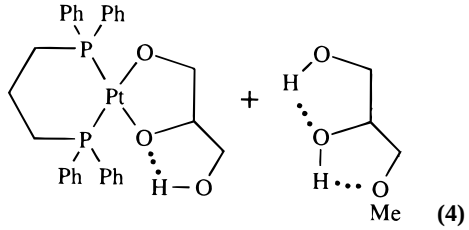

(4)

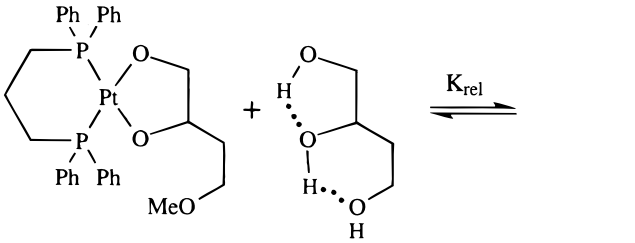

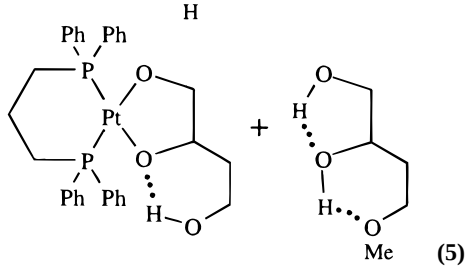

(5)

below 6 mM.[18] Phenol is also a sufficiently good HBD that 75−95% of the full hydrogen bond titration curve (vide infra) can be obtained at reasonably low acceptor concentrations ($[Pt]_{max} \leq 20$ mM, $[OPPh_3]_{max} \leq 0.3$ M). Triphenylphosphine oxide was chosen as a HBA comparison reference for the present studies since it is well-known to be one of the strongest neutral hydrogen bond acceptors.[16]

The choice of platinum complex was more difficult. The dppp auxiliary ligand was chosen for the studies since our most extensive set of carbohydrate complexation data is available for this series of complexes.[1] Aside from adequate solubility of the HBA, the other compelling criterion is that the HBD molecule, in this case phenol, must not undergo diolate−phenol exchange reactions at the concentrations used for the hydrogen-bonding studies. For example, (dppp)Pt(ethane-1,2-diolate) was observed to undergo partial conversion to (dppp)Pt$(OPh)_2$ on treatment with a modest excess of phenol.[19] The more electron-deficient diol, phenylethane-1,2-diol ($PedH_2$), has a factor of 8 better binding constant to (dppp)Pt than does ethane-1,2-diol.[1] This proved adequate to prevent significant phenol exchange from occurring; hence (dppp)Pt(Ped) was selected for study. (Exchange could also be circumvented by using a diol as the probe molecule, e.g., ethanediol with (dppp)Pt(ethanediolate), where exchange is a degenerate reaction. This course was decided against as diols are not nearly as well calibrated as phenol as hydrogen bond donors.)

Intermolecular hydrogen bond strengths can be determined by titrations, which can be monitored, e.g., by calorimetry or by NMR or IR spectroscopies.[14,15,20−22] Thermodynamic studies

(13) Parshall, G. W.; Ittel, S. D. *Homogeneous Catalysis: The Applications and Chemistry of Catalysis by Soluble Transition Metal Complexes;* 2nd ed.; Wiley: New York, 1992.
(14) Murthy, A. S. N.; Rao, C. N. R. *Appl. Spectrosc. Rev.* **1968**, *2*, 69−191.
(15) Joesten, M. D.; Schaad, L. J. *Hydrogen Bonding*; Marcel Dekker, Inc.: New York, 1974.
(16) Kamlet, M. J.; Abboud, J.-L. M.; Abraham, M. H.; Taft, R. W. *J. Org. Chem.* **1983**, *48*, 2877−2887.
(17) Gramstad, T.; Becker, E. D. *J. Mol. Struct.* **1970**, *5*, 253−261.
(18) Aksnes, G.; Gramstad, T. *Acta Chem. Scand.* **1960**, *14*, 1485−1494.
(19) Cook, G. K. Unpublished observations.
(20) Pimentel, G. C.; McClellan, A. L. *Annu. Rev. Phys. Chem.* **1971**, *22*, 347−385.

based on OH stretching vibrations in the infrared have often been used, but careful attention to methodology is required, i.e., use of integrated, temperature-dependent extinction coefficients, and often deconvolution of overlapping bands due to the free and bound species, which may each also exhibit multiple peaks due to different rotational conformers or overtones of other vibrations.[20,23] The need to work at high dilution, to avoid complications due to phenol self-association, favors the use of high-sensitivity ^{1}H NMR. Furthermore, changes in NMR OH chemical shifts due to hydrogen bonding, though exchange averaged, are readily and accurately quantified; therefore, this method was selected.

(b) Data Analysis. In the ^{1}H NMR method, the chemical shift of the phenol OH proton is monitored as a dilute phenol solution (~6 mM) is titrated with a concentrated solution of the hydrogen bond acceptor (~0.5 M for $OPPh_3$, ~25 mM for Pt). The observed exchange-averaged OH chemical shift, δ_{obs}, at each point in, e.g., the Ph_3PO titration (eq 1), is given by[24]

$$\delta_{obs} = \delta_o[PhOH]/[PhOH]_{tot} + \delta_1[Ph_3PO{\cdot}PhOH]/[PhOH]_{tot} = \delta_o + \Delta\delta_1[Ph_3PO{\cdot}PhOH]/[PhOH]_{tot} \quad (6)$$

where δ_o is the chemical shift of free phenol, δ_1 is the limiting chemical shift of the OH proton in the $Ph_3PO{\cdot}PhOH$ adduct, $[PhOH]_{tot} = [PhOH] + [Ph_3PO{\cdot}PhOH]$, and $\Delta\delta_1 = (\delta_1 - \delta_o)$. The equilibrium constant expression for eq 1, $K_1 = [Ph_3PO{\cdot}PhOH]/[Ph_3PO][PhOH]$, can be solved for $[Ph_3PO{\cdot}PhOH]$ in terms of K_1, $[Ph_3PO]_{tot}$, and $[PhOH]_{tot}$. Substitution of this expression into eq 6 gives a quadratic equation for δ_{obs} as a function of three knowns, $[Ph_3PO]_{tot}$, $[PhOH]_{tot}$, and δ_o, and two unknowns, K_1 and $\Delta\delta_1$ (see Appendix).[15,25]

Similar definitions and equations can be written for the Pt system (eq 2), except that a second equilibrium constant, K_2, and limiting chemical shift, δ_2, corresponding to eq 3 were ultimately needed (vide infra). In this case, the observed exchange-averaged phenol ^{1}H NMR OH chemical shift can be expressed as the sum of the mole percent of each of the three phenol species present at equilibrium (PhOH, (dppp)Pt(Ped)·(PhOH), (dppp)Pt(Ped)·$(PhOH)_2$) times their corresponding chemical OH shifts, δ_o, δ_1, and δ_2, respectively. The concentrations of the three phenol species are in turn derived from the equilibrium constant expressions for eqs 2 and 3 via a cubic equation (see Appendix for details). These two equations have a total of three knowns (the total phenol and Pt concentrations $[PhOH]_o$ and $[Pt]_o$, and the free phenol chemical shift δ_o), two linear unknowns ($\Delta\delta_1 = \delta_1 - \delta_o$ and $\Delta\delta_2 = \delta_2 - \delta_o$) and two nonlinear unknowns (K_1 and K_2). (It should be noted that the chemical shift δ_1 is actually a weighted average of up to four isomeric monophenol hydrogen bonded adducts, i.e., one with phenol bound to the Pt diolate oxygen adjacent to the CH_2 group and one with phenol bound to the Pt diolate oxygen adjacent to the CHPh group, each of which can have the phenol *syn* or *anti* to the diolate phenyl group. The chemical shift δ_2 is similarly a weighted average of isomers. The derived *K*'s, $\Delta H°$'s, and $\Delta S°$'s are therefore also isomeric averages.)

A number of methods are available for analyzing monoassociation hydrogen-bonding titration data with respect to the δ_{obs} equation, the simplification of Scatchard[26] having been used for most prior related studies of alcohol−metal alkoxide interactions,[27−31] aside from a couple calorimetric studies.[27,32] The relative merits of several of these methods, and factors to be considered in their application, have been discussed in some detail,[33] including complications due to multiple equilibria,[34] such as those potentially present here. Key issues in the use of a Scatchard plot are (1) the need to work at high HBA to HBD ratios to permit the approximation that $[HBA]_o - [HBA{\cdot}HBD] \approx [HBA]_o$ (where $[HBA]_o$ is the total concentration of all HBA species), (2) the need to cover a wide range ("at least 75%"[33]) of the theoretical span of 0.0−1.0 of the "saturation factor", i.e., the ratio of $[HBA{\cdot}HBD]/[HBD]_o$, in order to look for deviations from 1:1 complexation and other nonideal behaviors such as HBD dimerization, and (3) the fact that much larger errors arise at low (<0.2) and high (>0.8) saturation ranges. Prior studies of alcohol−metal alkoxide interactions have suffered from serious deviations from these criteria, i.e., situations where the data reported indicate that $[HBA{\cdot}HBD] \approx 0.5[HBA]_o$[28,29] or that the saturation factor ranges covered by the four to six data points are only 0.29−0.53 or 0.53−0.76 at best[30] to 0.98−1.00 at worst.[28] Another matter of some concern is self-association of the HBD since this is not discussed in these articles and in some cases $[HBD]_o > 50$ mM,[28,29] which is above the concentration at which self-association can usually be ignored. Also apparently overlooked in these prior metal alkoxide hydrogen-bonding studies are corrections for temperature effects on concentrations, which for dichloromethane amounts to 7% over the range 270−320 K (see Experimental Section). Failure to correct for this can lead to comparable-sized systematic errors in $\Delta H°$.[25]

We have addressed these issues in the present study in several ways. First, titrations were conducted over as large a middle fraction of saturation factor as readily accessible, i.e., from ~0.2−0.9 for $OPPh_3$ + PhOH and, for (dppp)Pt(Ped) + PhOH, from ~0.1−0.85 for low-temperature runs and from ~0.1−0.75 for high-temperature runs. Second, we attempted to minimize multiple association phenomena involving both phenol aggregation and formation of (dppp)Pt(Ped)·$(PhOH)_2$ species by working at $[PhOH] \leq 6$ mM. For the Pt system described by eqs 2 and 3, the equilibrium constant expression for eq 3 can be rewritten as in eq 7:

$$[Pt{\cdot}(PhOH)_2]/[Pt{\cdot}(PhOH)] = K_2[PhOH] \quad (7)$$

hence, a low [PhOH] will also minimize formation of (dppp)Pt(Ped)·$(PhOH)_2$. Third, we used nonlinear least-squares fits of sets of 8−20 titration data points to the exact δ_{obs} equations; thus, we did not need to resort to approximations such as those employed in the derivation of the Scatchard equation described

(21) Tucker, E. E.; Lippert, E. In *The Hydrogen Bond. Recent Developments in Theory and Experiments. II. Structure and Spectroscopy*; Schuster, P., Zundel, G., Sandorfy, C., Eds.; North-Holland Publishing Co.: New York, 1976; Vol. II, pp 793−830.
(22) Joesten, M. D. *J. Chem. Educ.* **1982**, *59*, 362−366.
(23) Hadzi, D.; Bratos, S. In *The Hydrogen Bond. Recent Developments in Theory and Experiments. II. Structure and Spectroscopy*; Schuster, P., Zundel, G., Sandorfy, C., Eds.; North-Holland Publishing Co.: New York, 1976; Vol. II, pp 567−611.
(24) Sherry, A. D. In *The Hydrogen Bond: Recent Developments in Theory and Experiments. III. Dynamics, Thermodynamics and Special Systems*; Schuster, P., Zundel, G., Sandorfy, C., Eds.; North-Holland Publishing Co.: New York, 1976; Vol. III, pp 1201−1224.
(25) Wiley, G. R.; Miller, S. I. *J. Am. Chem. Soc.* **1972**, *94*, 3287−3293.
(26) Scatchard, G. *Ann. N.Y. Acad. Sci.* **1949**, *51*, 660.
(27) Kegley, S. E.; Schaverien, C. J.; Freudenberger, J. H.; Bergman, R. G.; Nolan, S. P.; Hoff, C. D. *J. Am. Chem. Soc.* **1987**, *109*, 6563−6565.
(28) Kim, Y.-J.; Osakada, K.; Takenaka, A.; Yamamoto, A. *J. Am. Chem. Soc.* **1990**, *112*, 1096−1104.
(29) Osakada, K.; Kim, Y.-J.; Yamamoto, A. *J. Organomet. Chem.* **1990**, *383*, 303−317.
(30) Alsters, P. L.; Baesjou, P. J.; Janssen, M. D.; Kooijman, H.; Sicherer-Roetman, A.; Spek, A. L.; van Koten, G. *Organometallics* **1992**, *11*, 4124−4135.
(31) Kapteijn, G. M.; Dervisi, A.; Grove, D. M.; Kooijman, H.; Lakin, M. T.; Spek, A. L.; van Koten, G. *J. Am. Chem. Soc.* **1995**, *117*, 10939−10949.
(32) Osakada, K.; Kim, Y.-J.; Tanaka, M.; Ishiguro, S.-i.; Yamamoto, A. *Inorg. Chem.* **1991**, *30*, 197−200.
(33) Deranleau, D. A. *J. Am. Chem. Soc.* **1969**, *91*, 4044−4049.
(34) Deranleau, D. A. *J. Am. Chem. Soc.* **1969**, *91*, 4050−4054.

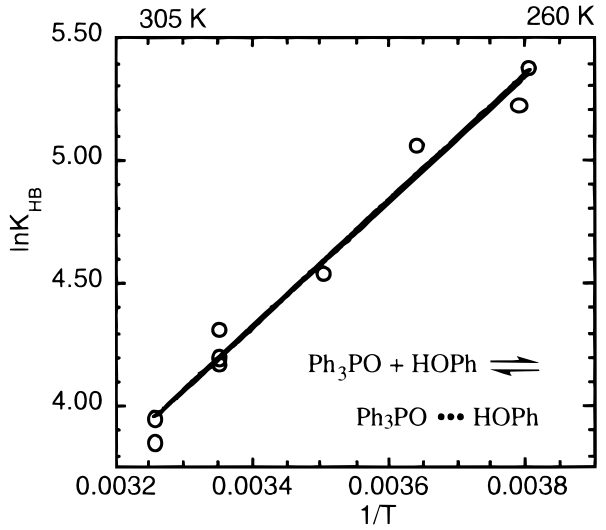

Figure 2. Van't Hoff plot for phenol−triphenylphosphine oxide hydrogen bonding; $\Delta H^\circ = -5.1 \pm 0.3$ kcal/mol and $\Delta S^\circ = -8.8 \pm 1.0$ eu.

Table 1. Hydrogen-Bonding Association Constants and NMR Complexation Chemical Shifts for Phenol + Triphenylphosphine Oxide in CD_2Cl_2

T/K	δ_o/ppm	$\Delta\delta$/ppm	K_{HB}/M^{-1}
263	4.96	5.28 ± 0.01	215 ± 6
264	4.93	5.32 ± 0.01	185 ± 6
275	5.03	5.17 ± 0.01	158 ± 5
285	4.86	5.31 ± 0.01	93 ± 3
298	4.93	5.22 ± 0.01	66 ± 2
298	4.82	5.34 ± 0.01	65 ± 2
298	4.82	5.24 ± 0.02	75 ± 3
307	4.79	5.33 ± 0.01	52 ± 1
307	4.85	5.30 ± 0.01	47 ± 1

above. For the system $OPPh_3$ + PhOH (eq 1), this was readily accomplished using either the commercial KaleidaGraph package[35] or custom routines written for MatLab.[36] The resulting least-squares optimized equilibrium constants, complexation OH chemical shift changes, and their Monte Carlo estimated errors (vide infra) are listed in Table 1. The corresponding van't Hoff plot and derived hydrogen-bonding enthalpy and entropy parameters are given in Figure 2.

For the Pt system, initial attempts to treat the system as a single-association problem (eq 2 only) gave reasonable fits but the plots showed small but systematic deviations between the observed data points and the calculated curve, especially at low temperatures (cf. Figure 3a). Furthermore, when δ_o was included as an unknown in this single-association model, the resulting fitted value of δ_o was farther downfield than that experimentally observed. The errors in fitting the observed data to this single association model were consistent with significant contributions from the doubly associated species (dppp)Pt(Ped)·-$(PhOH)_2$ (eq 3) being present, despite attempts to minimize its formation by appropriate experimental design.

This finding was not completely unanticipated based on preliminary experiments using ^{31}P NMR instead of ^{1}H NMR to monitor the hydrogen-bonding titration curve.[1,37] Such ^{31}P NMR experiments offered the advantage of multiple "observed's" (i.e., two ^{31}P chemical shifts for the nonequivalent P atoms in (dppp)Pt(Ped) and two Pt−P coupling constants), which in some cases also exhibit shifts of opposite signs for the primary and secondary association (cf. the titration plot

(35) Abelbeck Software, distributed by Synergy Software, 2457 Perkiomen Ave., Reading, PA 19606.
(36) The Math Works, Inc., 24 Prime Park Way, Natick, MA 01760.
(37) Voss, E. J.; Brunkan, N. M. Unpublished observations.

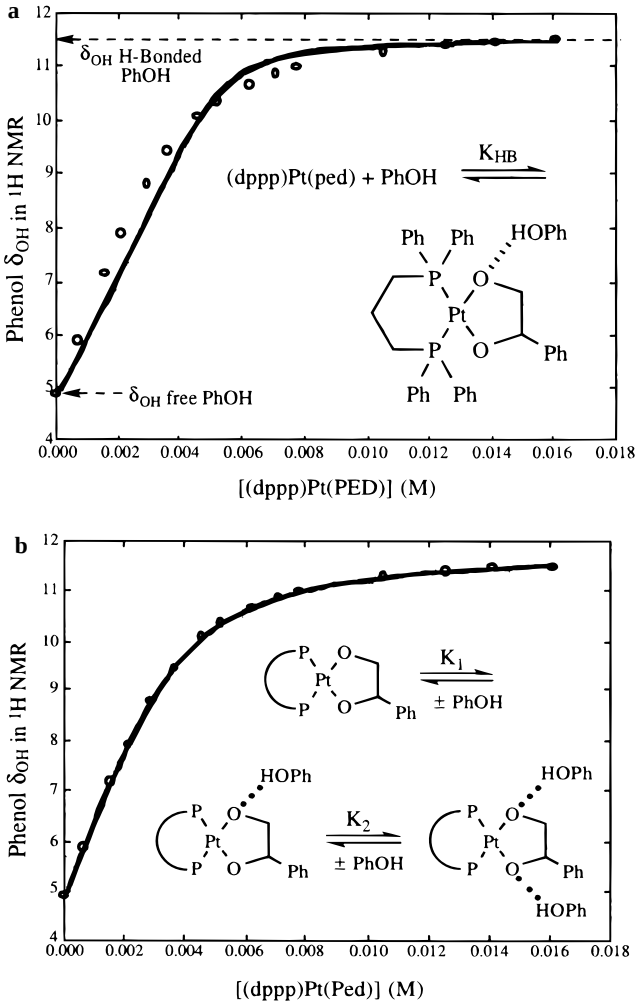

Figure 3. Fit of phenol−(dppp)Pt(Ped) hydrogen bond association at 267 K to (a) a single equilibrium constant model (eq 2) ($K_{HB} = 5101$ M^{-1}, $\Delta\delta = 6.7$ ppm) and (b) a double-association model (eqs 2 and 3) ($K_1 = 1843 \pm 113$ M^{-1}, $K_2 = 225 \pm 25$ M^{-1}, $\Delta\delta_1 = 6.90$ ppm, and $\Delta\delta_2 = 6.13$ ppm).

shown in Figure 4 of ref 1). Despite the obvious data-fitting advantages of this approach, it was ultimately rejected in favor of monitoring the single observed change in phenol OH chemical shift by ^{1}H NMR. The use of ^{31}P NMR would have required titrating the Pt complex with added phenol, inevitably leading to solution concentrations where phenol self-association would interfere. With ^{1}H NMR, the titration is done in the opposite manner; hence, the phenol concentration can be kept essentially fixed at a low value, further facilitated by the significantly higher sensitivity of ^{1}H over ^{31}P NMR. Thus with more data analysis effort, it appeared that it might be possible to extract both K_1 and K_2 from the ^{1}H NMR Pt−PhOH titration data. We therefore employed MatLab least-squares routines to simultaneously fit the linear variables $\Delta\delta_1$ and $\Delta\delta_2$ in the equation for δ_{obs} (eq A5 in the Appendix) together with the nonlinear variables K_1 and K_2 corresponding to the dual equilibria defined by eqs 2 and 3 (see Appendix). The resulting temperature-dependent equilibrium constants and calculated shifts on complexation are listed in Table 2a. Figure 3b shows the improved fit to the titration data. In order to assess the validity and quality of these multiparameter fits, a Monte Carlo error analysis routine was also implemented in MatLab (see Appendix), giving the results also included in Table 2. This analysis accounted for both systematic errors in the starting Pt and PhOH stock solutions (±2%) and for subsequent random syringing errors (±1%) during the titrations.

Table 2. Hydrogen-Bonding Association Constants and NMR Complexation Chemical Shifts for Phenol + (dppp)Pt(Ped) in CD_2Cl_2

(a) Fit to $\Delta\delta_1$, $\Delta\delta_2$, K_1, and K_2

T/K	δ_o/ppm	$\Delta\delta_1$/ppm	$\Delta\delta_2$/ppm	K_1/M^{-1}	K_2/M^{-1}
266.9	4.89	6.90 ± 0.01	6.1 ± 0.3	1843 ± 113	225 ± 25
266.9	4.89	6.91 ± 0.01	5.8 ± 0.2	1839 ± 64	245 ± 19
279.8	4.86	6.86 ± 0.02	6.7 ± 0.4	891 ± 42	103 ± 11
280.4	4.86	6.80 ± 0.02	6.5 ± 0.3	955 ± 34	121 ± 14
298.0	4.82	6.93 ± 0.05	9.5 ± 3.7	368 ± 29	28 ± 11
298.0	4.82	6.71 ± 0.04	6.0 ± 0.7	476 ± 48	48 ± 11
307.2	4.79	6.74 ± 0.05	5.9 ± 1.7	328 ± 29	43 ± 13
307.2	4.79	6.68 ± 0.03	4.7 ± 0.4	381 ± 22	78 ± 16
320.8	4.76	6.86 ± 0.42	17 ± 2020	173 ± 53	8 ± 24
320.8	4.76	6.82 ± 0.16	21 ± 126	177 ± 31	5 ± 17

(b) Fit to $\Delta\delta_1$, K_1, and K_2; $\Delta\delta_2$ Fixed at 6.0

T/K	$\Delta\delta_1$/ppm	K_1/M^{-1}	K_2/M^{-1}
266.9	6.90 ± 0.01	1903 ± 69	240 ± 29
266.9	6.90 ± 0.02	1799 ± 51	220 ± 29
279.8	6.86 ± 0.02	964 ± 27	136 ± 20
280.4	6.80 ± 0.02	989 ± 26	147 ± 15
298.0	6.86 ± 0.02	421 ± 12	54 ± 6
298.0	6.71 ± 0.03	476 ± 19	48 ± 6
307.2	6.74 ± 0.03	326 ± 12	42 ± 4
307.2	6.70 ± 0.03	343 ± 13	43 ± 6
320.8	6.71 ± 0.05	199 ± 9	22 ± 5
320.8	6.68 ± 0.04	199 ± 8	18 ± 4

For the low-temperature data (T = 267 and 280 K), it is clear that all four parameters are meaningfully fit (<10% error), but at higher temperatures (e.g., 321 K), the fit of K_2 and especially $\Delta\delta_2$ becomes meaningless. This is not surprising since at low temperatures it can be shown from eq 7 and the values of K_2 and [PhOH] that roughly equal quantities of both (dppp)Pt(Ped)·(PhOH) and (dppp)Pt(Ped)·$(PhOH)_2$ are present for the early titration data points, thereby readily allowing all parameters to be effectively fit. At high temperatures, where K_2 is much smaller, there is now relatively little (dppp)Pt(Ped)·$(PhOH)_2$ present; hence it is not possible to fit K_2 and $\Delta\delta_2$ separately. This is because at these low degrees of association for K_2 the corresponding titration plot is essentially linear, precluding separate determination of the nonlinear component; thus only the product $K_2\Delta\delta_2$ can be meaningfully fit, 143 ± 72 and 120 ± 24 for the two 321 K runs.

The observed temperature dependences of δ_o and the well-determined $\Delta\delta_1$'s from 267−320 K are both small, <0.2 ppm, compared to the total shift on complexation of ∼6−7 ppm. Based on this observation, the two 267 K titration data sets were fit varying all four unknowns (K_1, K_2, $\Delta\delta_1$, $\Delta\delta_2$) and then all the data sets were refit varying only K_1, K_2, and $\Delta\delta_1$, keeping $\Delta\delta_2$ fixed at the value of 6.0 calculated from the 267 K data sets. This analysis resulted in the final equilibrium constant data given in Table 2b. A test of the potential error in this approach was made in which the 320 K data set was fit with a fixed $\Delta\delta_2$ value of 5.8. This gave values for K_1 and K_2 that were within 1 and 3%, respectively, of those using the fixed $\Delta\delta_2$ value of 6.0. The validity of this approach and the overall quality of the hydrogen-bonding association constant data are further demonstrated by the precision of the resulting dual van't Hoff plot for both K_1 and K_2 (Figure 4). Attempts to carry out analogous studies in pyridine were thwarted by the lack of a significant phenol OH chemical shift change as a function of added platinum diolate complex concentration, presumably due to competitive hydrogen bonding of the phenol to the neat pyridine solvent.

(c) Hydrogen-Bonding Thermodynamics. An extensive tabulation[16] of the Kamlet and Taft β scale of HBA basicities[38]

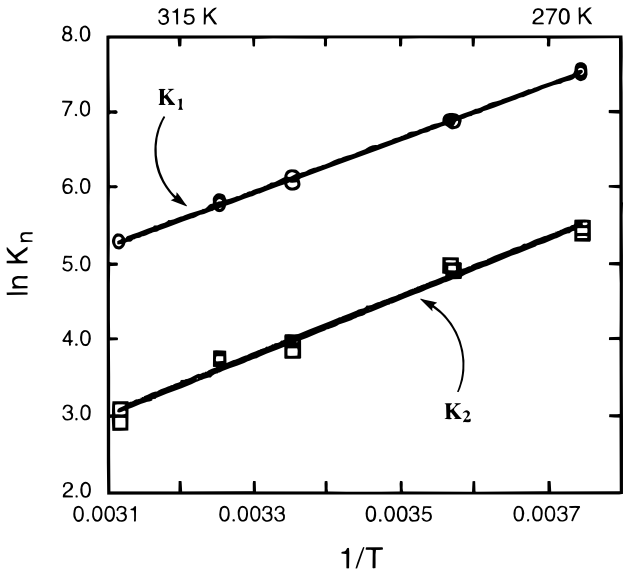

Figure 4. Van't Hoff plot for phenol−(dppp)Pt(Ped) hydrogen-bonding interactions: $\Delta H_1^\circ = -7.0 \pm 0.1$ kcal/mol, $\Delta H_2^\circ = -7.7 \pm 0.4$ kcal/mol; $\Delta S_1^\circ = -11.3 \pm 0.4$ eu, $\Delta S_2^\circ = -17.8 \pm 1.2$ eu.

of a wide variety of hydrogen bond acceptors shows that triphenylphosphine oxide (β = 0.94) is one of the strongest HBAs, even better than amides, amines, and sulfoxides ($\beta \approx$ 0.6−0.8). A previous study of hydrogen bonding of phenol with $OPPh_3$ in carbon tetrachloride solution by near-infrared spectroscopy gave K_{HB} = 1055 M^{-1} at 293 K[18], a ΔH° of −6.7 kcal/mol, and a ΔS° of −8.7 eu.[39] Our values in dichloromethane solution, K_{HB}^{293} = 71 M^{-1} (calcd), $\Delta H^\circ = -5.1 \pm$ 0.3 kcal/mol, and $\Delta S^\circ = -8.8 \pm 1.0$ eu, correspond to weaker association, probably resulting from stabilization of the reactants by the more polar solvent.[40,41] A very similar solvent difference has been seen for hydrogen bonding of *p*-fluorophenol with triphenylphosphine oxide: K^{298} = 1456 ± 80 M^{-1} in carbon tetrachloride[42] and 80 M^{-1} in dichloromethane.[41]

Compared to $OPPh_3$, the Pt diolate complex (dppp)Pt(Ped) interacts even more strongly with phenol, the first hydrogen-bonding association constant K_1 in dichloromethane being ∼1 order of magnitude higher (K_1 (Pt) = 450 M^{-1} vs K_{HB} ($OPPh_3$) = 70 M^{-1} at 298 K). This stronger association is due to a more negative enthalpy of association $\Delta H_1^\circ = -7.0 \pm 0.1$ kcal/mol, compared with $\Delta H^\circ = -5.1 \pm 0.3$ kcal/mol for Ph_3PO, making this Pt diolate complex among the strongest neutral HBA species. The entropy of association, $\Delta S_1^\circ = -11.3 \pm 0.4$ eu, is comparable to that of Ph_3PO (−8.8 ± 1.0 eu). Related phenol adducts of several Pd phenoxide complexes have been reported to have similar association enthalpies (−4 to −7 kcal/mol),[4] while the electron-rich complex $Rh(PMe_3)_3(p\text{-}OC_6H_4Me)$ is reported to have a $p\text{-}HOC_6H_4Me$ hydrogen-bonding association enthalpy of −14.0 ± 0.4 kcal/mol.[27] This latter result was obtained by calorimetry in cyclohexane, the value decreasing to −11.4 ± 0.5 kcal/mol in benzene, again showing the significant effect of solvent on these interactions.

A unique aspect of the present study is the accurate evaluation of both the first *and* second hydrogen-bonding phenol associa-

(38) Kamlet, M. J.; Taft, R. W. *J. Am. Chem. Soc.* **1976**, *98*, 377−383.

(39) Values from: Joesten, M. D.; Drago, R. S. *J. Am. Chem. Soc.* **1962**, *84*, 3817−3821 (derived from K_{HB} values at 273 and 323 K given in ref 18).

(40) Compare study of solvent dependence of hydrogen bonding between phenol and pyridine: Spencer, J. N.; Andrefsky, J. C.; Grushow, A.; Naghdi, J.; Patti, L. M.; Trader, J. F. *J. Phys. Chem.* **1987**, *91*, 1673−1674.

(41) Joris, L.; Mitsky, J.; Taft, R. W. *J. Am. Chem. Soc.* **1972**, *94*, 3438−3442.

(42) Gurka, D.; Taft, R. W. *J. Am. Chem. Soc.* **1969**, *91*, 4794−4801.

tion thermodynamics for (dppp)Pt(Ped). The second association constant K_2 is ~1 order of magnitude smaller than the first (cf. Table 2). This decrease is due entirely to the more negative entropy, $\Delta S_2^\circ = -17.8 \pm 1.2$ eu, the association enthalpy $\Delta H_2^\circ = -7.7 \pm 0.4$ kcal/mol being essentially identical to ΔH_1° (-7.0 ± 0.1) within experimental error. This entropic difference of 6.5 eu is significantly greater than the R ln 2 (1.4 eu) statistical difference expected due to the availability of two Pt diolate oxygens for the first interaction but only one for the second interaction (assuming that hydrogen bonding of two phenols to a single Pt oxygen is significantly less favorable than to two different oxygens). A statistical factor of R ln 4 (2.8 eu) is possible if the second phenol association must be correlated with the first, e.g., one phenol above the diolate metallacycle plane on one oxygen and the second phenol below the plane on the opposite oxygen. There may also be greater hindrances to phenyl group rotations in the bis(phenol) adduct, both in the associated phenols and the diolate and phosphine ligands. This entropic difference in K_1 and K_2 observed here casts doubt on the assumption invoked in analysis of phenol hydrogen bonding to *trans*-Pd(L)$_2$(OPh)$_2$ complexes that K_1 and K_2 in those systems were equal.[30] The equivalence of ΔH_1 and ΔH_2 is noteworthy, indicating that hydrogen bond formation at one diolate oxygen has very little electronic effect on the other diolate oxygen.[43]

A linear enthalpy−entropy correlation[15,20] has been reported for hydrogen bonding of alcohols and late-metal alkoxide complexes: $\Delta S^\circ = m\Delta H^\circ + b$, where $m = 4.04$ and $b = 13.0$ (ΔH° in kcal/mol; ΔS° in eu).[31] Using our observed ΔH° values for hydrogen bonding of phenol to (dppp)Pt(Ped) and this equation, calculated entropy values of $\Delta S_1^\circ = -15$ eu and $\Delta S_2^\circ = -18$ eu are obtained. The latter is in excellent agreement with the observed ΔS_2° of -17.8 ± 1.2. The former differs from the observed value of -11.3 ± 0.4 eu by 4 eu. This discrepancy is significantly greater than any of the other data points in the literature plot (Figure 5 of ref 31), probably due to the favorable two(four)-site entropic statistical factor present in this diolate complex not accounted for by the standard enthalpy−entropy correlation. (The literature $\Delta S^\circ/\Delta H^\circ$ correlation includes an L$_2$Pd(OPh)$_2$ complex that might have a similar favorable entropic factor, but this factor may have been "removed" by the assumption used for analyzing the Pd−phenol adducts that the mono- and diadduct K's were equal. This may explain the observation that this data point is significantly off the correlation line in the opposite direction.)

Substituting the linear expression for ΔS° in terms of ΔH° into the standard expression $\Delta G^\circ = \Delta H^\circ - T\Delta S^\circ$ yields $\Delta G^\circ = \Delta H^\circ - T(m\Delta H^\circ + b) = \Delta H^\circ(1-mT) - bT$ (T in K/1000); thus, for hydrogen bonding of alcohols to late-metal alkoxides at room temperature, $\Delta G^\circ = -0.20\Delta H^\circ - 3.87$. The small magnitude of the coefficient of ΔH° indicates that ΔG°, and hence K_{HB}, is almost insensitive to the enthalpic strength of the metal-alkoxide hydrogen bond, ΔG° predicted to change by only 2 kcal/mol over the full 0−10 kcal/mol range of typical hydrogen bond strengths. Thus, the strongest ($\Delta H^\circ = -8.3$ kcal/mol)[44] and weakest ($\Delta H^\circ = -4.1$ kcal/mol)[45] metal−alkoxide hydrogen bonds for which full thermodynamic data have been reported (entries 1 and 6 in Table 3 and Figure 5 of ref 31) have K_{HB}'s that experimentally differ by only a factor of 2. Furthermore, as suggested by the negative sign of the coefficient of ΔH° in the empirical expression above, the *weaker* hydrogen bond (based on ΔH) is observed to have the *larger* K_{HB}! This striking result contrasts with the situation found for the association of phenol with various classes of organic bases, for which tabulations show that $0.47 < m < 3.32$ (and $-6.8 < b < +5.4$);[46] hence the ΔH° coefficient ($1-mT$) is positive at room temperature for all these systems, implying an increasing K_{HB} with increasing hydrogen bond enthalpy.

Further examination of these tables reveals that not only are ΔH° and ΔS° linearly correlated within families of compounds but that the constants for those correlations are correlated. Thus a plot of m vs b for the data from Tables 4-18 and 4-19 of ref 46, together with the values of m and b for metal alkoxides, can be fit to a straight line of the form $m = 0.14b + 2.27$ with a correlation coefficient of 0.79 for 41 data points (Figure S1, Supporting Information), correlation probability >99.9%. The physical basis of this secondary correlation is not immediately apparent.

Intramolecular Studies. (a) Experimental Design. Quantitative measurement of the strength of intramolecular hydrogen bonds is much more difficult than for intermolecular hydrogen bonds since it cannot be accomplished with calorimetry or titration-type experiments. The magnitude of differences in stretching vibration frequencies for free and intramolecular hydrogen bonded OHs provides qualitative information on this phenomenon, but quantification can be problematic.[23,47,48] The solution composition cannot be directly determined by integration of the corresponding IR bands since the molar extinction coefficients cannot be independently measured, nor assumed to be equal, and can only be estimated from model compounds, requiring very careful attention to methodology.[48,49] Rapid exchange on the NMR time scale of free and associated OHs precludes determination by NMR integration techniques at normally accessible temperatures. Accurate characterization of these weak interactions (~3−10 kcal/mol) by quantum mechanical methods is also difficult for all but the smallest molecules, and the effects of solvation are even harder to compute.[50]

The present system appeared to offer a unique opportunity for examination of intramolecular hydrogen bond strengths based on a complexation competition reaction between two appropriately chosen diols, as illustrated in eqs 4 and 5. In dilute solutions in nonHBA solvents (<5 mM to avoid intermolecular hydrogen bonding), both the free triol and its corresponding monomethylated derivative would be expected to form two intramolecular hydrogen bonds (though for glycerol there are two statistical ways to do so). Making the defensible assumptions that the hydrogen bond acceptor strengths of an OH and an OMe group are comparable within fractions of a kilocalorie per mole[51] and that the inherent Pt complexation strengths of the triol and its methylated derivative should be essentially identical (again aside from the cancelling statistical factor of 2 for glycerol), the thermodynamics of K_{rel} (eqs 4 and 5) then correspond to those of formation of the intramolecular Pt−O···H hydrogen bond. In a HBA solvent such as pyridine, however, the third, free hydroxyl group in the triol would be expected to form an intermolecular hydrogen bond to the solvent (eq 8). (The two intramolecular hydrogen bonds in the triol and methoxydiol may be disrupted by intermolecular hydrogen-bonding interactions with HBA solvents, but these interactions will cancel out in eq 8.) In this case, the reaction energetics for

(43) Compare similar results for multiple hydrogen bonding in *o*-hydroxyl-substituted benzoic acids: Shan, S.; Herschlag, D. *J. Am. Chem. Soc.* **1996**, *118*, 5515−5518.
(44) Pd(Me$_2$NCH$_2$CH$_2$NMe$_2$)(Me)(OCH(CF$_3$)$_2$)·HOCH(CF$_3$)$_2$ in CDCl$_3$.
(45) Pd(Me$_2$PCH$_2$CH$_2$PMe$_2$)(Me)(OPh)·HOPh in CD$_2$Cl$_2$.
(46) See ref 15, pp 247−251.
(47) Tichy, M. *Adv. Org. Chem.* **1965**, *5*, 115−290.
(48) Aaron, H. S. *Top. Stereochem.* **1979**, *11*, 1−52.
(49) See: Beeson, C.; Pham, N.; Shipps, G. J.; Dix, T. A. *J. Am. Chem. Soc.* **1993**, *115*, 6803−6812 and references therein for recent studies.
(50) Cramer, C. J.; Truhlar, D. G. *J. Am. Chem. Soc.* **1994**, *116*, 3892−3900.
(51) Tse, Y.-C.; Newton, M. D.; Allen, L. C. *Chem. Phys. Lett.* **1980**, *75*, 350−356.

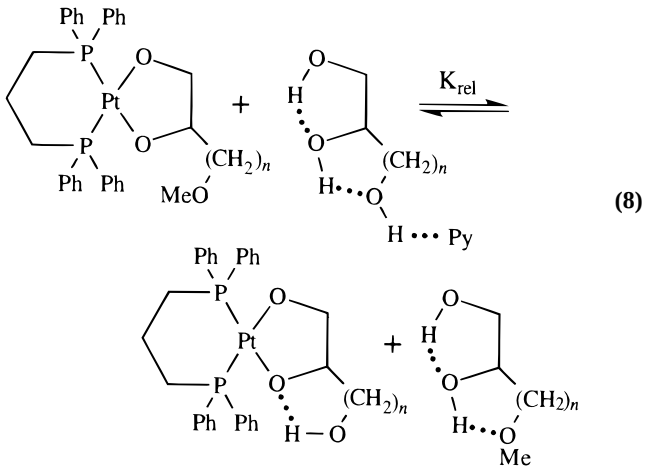

(8)

eq 8 reflect *the difference* in energies between intermolecular hydrogen bonding to the solvent of this hydroxyl in the triol and intramolecular hydrogen bonding of the same hydroxyl to the diolate oxygen in the Pt complex.

(b) Data Analysis. Analysis of the data from the competition reactions is simplified by the fact that the K_{rel}'s are dimensionless; hence, only the relative concentrations of the various components are needed. In principle, these could be obtained from ^{1}H NMR, but in practice there are too many signal overlaps for this to be effective. Instead, ^{31}P NMR was used to determine the relative concentrations of the two Pt species in each equilibrium. Combining this information with the known moles of starting materials and the reaction stoichiometries, the relative concentrations of the free diols and triols can be readily calculated for each equilibrium. Very accurate integrations are needed (±1−2%) because of the propagation of integration errors (twice in the numerator and twice in the denominator) and the involvement of small differences of large numbers in some cases. This level of precision and accuracy was obtained through the acquisition of high-S/N spectra with good digital sampling across the peaks, careful spectral phasing, slope and bias corrections, and employing tests for potential errors due to differences in relaxation times and nuclear Overhauser effects (see Experimental Section).

The largest source of error in these experiments was encountered for equilibria measured in dichloromethane. The Pt diolate complexes undergo slow reaction with this solvent to form (dppp)$PtCl_2$ and 1,3-dioxolanes, derived from net displacement of chloride from the CD_2Cl_2 by the diolate anion (eq 9), demonstrating again the high basicity of the diolate

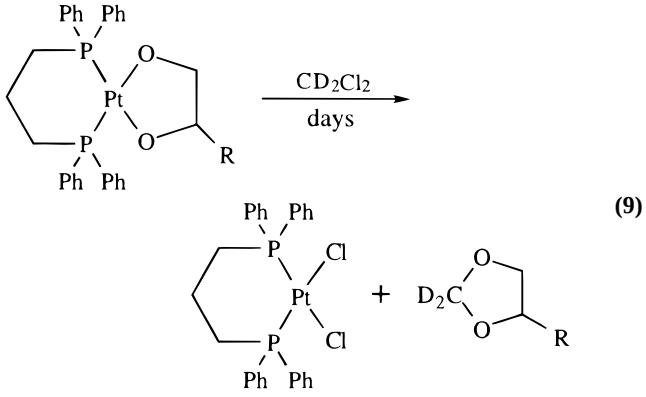

(9)

oxygen atoms. The major source of error introduced by this decomposition is the inability to accurately calculate the free diol/triol concentrations. While the amount of (dppp)$PtCl_2$ formed indicates how much total diol/triol is consumed by decomposition, it was not readily possible to determine the partitioning of this consumption between the diol and triol. In practice it was possible to achieve ligand exchange equilibration before substantial decomposition set in. Thus, we found that the use of worst case scenarios, i.e., all of the decomposition assumed to result from only the diolate or from only the triolate complex, gave acceptably small differences in the calculated K_{rel}'s (<20%). This level of precision in the calculated K_{rel}'s was further reinforced by measurement of the exchange equilibrium constants from both directions, conditions that should alter the relative contributions of the diol and triol to the decomposition products. The K_{rel}'s resulting from these studies, conducted in both dichloromethane and pyridine solution, are given in Table 3.

Table 3. Relative (dppp)Pt(II) Complexation Constants at 313 K for $HOCH_2CHOH(CH_2)_nCH_2OR$ (R = H vs R = Me)

n	solvent	K_{rel} derived from Pt(diolate) + triol	K_{rel} derived from Pt(triolate) + diol	ΔG^{313} (kcal/mol)
0	CD_2Cl_2	27/29[a]	25/28[a]	−2.05 ± 0.05
1	CD_2Cl_2	52/62[a]	55/63[a]	−2.52 ± 0.06
0	pyridine	2.7 ± 0.1	2.7 ± 0.1	−0.62 ± 0.03
1	pyridine	3.80 ± 0.04	3.7 ± 0.1	−0.82 ± 0.03

[a] The two values for K_{rel} are based on limiting assumptions with respect to correction for decomposition of the Pt complexes to (dppp)$PtCl_2$ (see text).

(c) Hydrogen-Bonding Strength in Pt Triolate Complexes. Before discussing the quantitative results, there are two issues to be considered. First, the quantity that we are interested in here, and the one that we have measured, is the net total energetics resulting from intramolecular hydrogen bond formation. This is not the same as the isolated hydrogen bond strength, since in an intramolecular hydrogen bond, much more so than in intermolecular hydrogen bond formation, there are other factors that contribute to the measured equilibrium, e.g., changes in nonbonded interactions elsewhere in the molecule.[52,53] Second, while it is tempting to conclude that the energetics of eq 4 represent hydrogen bond strengths for the five-membered ring shown and eq 5 those for the six-membered ring shown, this is only strictly true for metallacycle conformers having equatorially disposed hydroxyalkyl substitutents.[1] In axially substituted conformers, contributions from six-membered and seven-membered rings, respectively, are also possible via hydrogen bonding to the far oxygen in the diolate ligand (cf. Figure 1), rather than the near oxygen as illustrated in eqs 4 and 5 for simplicity. For the (dppp)Pt(butanetriolate) complex, Karplus-type J_{PtOCC} coupling constant analyses show that the hydroxyethyl substitutent is ∼50% equatorially disposed,[1] while for the (dppp)Pt(glycerolate) complex, the hydroxymethyl substituent is roughly 75:25 ax:eq. A more rigorous delineation of ring size effects might be experimentally achievable in a related monoalkoxy platinum system, e.g., (dppp)Pt(Y)($O(CH_2)_n$-OR) (R = H vs Me), in which the intramolecular hydrogen bond ring size would be unambiguous. This would appear to be feasible as $(Ph_2PCH_2CH_2PPh_2)Pt(CH_3)(OMe)$ is known and undergoes analogous exchange reactions,[54] but such a study was beyond the scope of the present work.

The net intramolecular hydrogen bond free energies, ΔG^{313} = −2.05 ± 0.05 and −2.52 ± 0.06 kcal/mol, observed in the two (dppp)Pt(triolate) complexes with different side-chain lengths (eqs 4 and 5, respectively), are both quite comparable

(52) Schuster, P. In *The Hydrogen Bond. Recent Developments in Theory and Experiments. I. Theory of the Hydrogen Bond*; Schuster, P., Zundel, G., Sandorfy, C., Eds.; North-Holland Publishing Co.: New York, 1976; Vol. I, p 123 ff.
(53) Dziembowska, T.; Szczodrowska, B.; Krygowski, T. M.; Grabowski, S. J. *J. Phys. Org. Chem.* **1994**, *7*, 142−146.
(54) Bryndza, H. E.; Fong, L. K.; Paciello, R. A.; Tam, W.; Bercaw, J. E. *J. Am. Chem. Soc.* **1987**, *109*, 1444−1456.

to those for the first and second intermolecular hydrogen bonds formed between (dppp)Pt(Ped) and phenol, $\Delta G_1^{313} = -3.5$ kcal/mol and $\Delta G_2^{313} = -2.1$ kcal/mol (calculated from the van't Hoff plot). The (dppp)Pt(triolate) intramolecular hydrogen bonds would be expected to have lower enthalpies than the intermolecular hydrogen bonds in (dppp)Pt(Ped)·HOPh, since the less acidic triolate hydroxyls should be poorer HBDs than phenol and because intramolecular hydrogen bonds cannot attain the optimal 180° O−H···O bond angle.[55] These enthalpic factors are partially compensated for by the favorable entropic chelate effect present with intramolecular hydrogen bonds compared to intermolecular association, leading to the observed comparable free energies for the two systems.

Attempts to accurately determine these intramolecular hydrogen-bonding enthalpies and entropies directly, from temperature-dependent K_{rel} measurements of the diol/triol exchange reactions, were thwarted by the decomposition reactions in dichloromethane. For the 4-methoxy-1,2-butanediol/1,2,4-butanetriol reaction in pyridine, however, the negligible change in K_{rel} observed between 40 and 90 °C indicates that $\Delta H°$ for intramolecular hydrogen bonding in the Pt triolate and for intermolecular hydrogen bonding of the free triol hydroxyl to pyridine must be nearly equal (cf. eq 8). We can estimate this enthalpy to be between −4 and −6 kcal/mol based on the enthalpies of the methanol−pyridine adduct in CCl_4 (−3.8 ± 0.1 kcal/mol[56]) and of the phenol−pyridine adduct in CH_2Cl_2 (−5.9 ± 0.2 kcal/mol[57]). The near equality of the enthalpies of the intramolecular Pt(triolate) and intermolecular triolate hydroxyl−pyridine hydrogen bonds follows from (1) the greater inherent HBA ability of the (dppp)Pt(diolate) system compared to pyridine ($\Delta H°_{HB} = -7.0$ kcal/mol for (dppp)Pt(Ped)·HOPh and −5.9 kcal/mol for Py·HOPh), compensated for by (2) the decreased hydrogen bond strength of the intramolecular bond due to geometric constraints and associated conformational interactions.

The most relevant prior study of high quality is that of α,ω-diol monomethyl ethers by Prabhumirashi and Jose.[58,59] They used IR spectroscopy to determine the thermodynamics of intramolecular hydrogen bonding in $HO(CH_2)_nOMe$ ($n = 2-4$) for which $\Delta G° = -1.41 \pm 0.3$, $+0.20 \pm 0.2$, and $+0.47 \pm 0.3$ kcal/mol for hydrogen bond ring sizes of five to seven, respectively, in carbon tetrachloride. This trend is opposite ours for the Pt triolate complexes, $\Delta G^{313} = -2.05 \pm 0.05$ and -2.52 ± 0.06 kcal/mol for increasing ring size. They also reported values for $\Delta H°$ of -3.5 ± 0.2, -3.6 ± 0.1, and -4.3 ± 0.2 kcal/mol and $\Delta S°$ of -7.0 ± 0.6, -12.4 ± 0.5, and -16.3 ± 0.5 eu. The enthalpies, which span a narrow range, are somewhat smaller than our estimated value of −4 to −6 kcal/mol for the enthalpy of intramolecular hydrogen bonding in the (dppp)Pt(1,2,4-butanetriolate) complex. This is consistent with the greater HBA ability of the Pt(diolates) compared to ethers, leading to more negative $\Delta H°$'s and hence the more negative $\Delta G°$'s observed for intramolecular hydrogen bonds in the Pt complexes compared to α,ω-alkoxy alcohols. The hydrogen bond entropies for the α,ω-alkoxy alcohols span a much larger range than their enthalpies and thus determine the trends in intramolecular hydrogen bond free energies in those complexes. It would appear that the opposite is true for the Pt(triolates), the more negative enthalpies expected for larger rings (due to more linear O−H···O bonds) dominating the same trends in entropies to produce the observed trend toward more negative free energies with increasing ring size.

While modest, these hydrogen bond free energies are sufficient to ensure that >95% of the (dppp)Pt(triolate) complex is present in the intramolecularly hydrogen-bonded form in dichloromethane, thereby generating good complexation selectivities, i.e., better than 85:15 for each triol over its analogous methoxydiol for a 1:1 mixture of triol and diol. The complexation selectivities in pyridine are somewhat smaller, i.e., ∼65:35, due to the much smaller exchange reaction free energies, $\Delta G^{313} = -0.62 \pm 0.03$ and -0.82 ± 0.03 kcal/mol for eqs 4 and 5, respectively. The difference between these values and those in dichloromethane (−2.05 and −2.52 kcal/mol, respectively) correspond to the triol hydroxyl−pyridine intermolecular hydrogen bond free energy, ∼−1.6 kcal/mol, comparable to that observed for MeOH·pyridine (-0.64 ± 0.02 kcal/mol in CCl_4[56]) and PhOH·Py (-1.69 ± 0.02 kcal/mol in CH_2Cl_2[60]). These results show that the diolate oxygens in the Pt complexes are sufficiently good HBAs that ∼75% of the Pt triolate complex is still present in the intramolecular hydrogen bonded form in the strong HBA pyridine solvent.

Interestingly, the rates of approach to equilibrium for eqs 4 and 5 at 40 °C were observed to be much faster in dichloromethane (hours) than in pyridine (days). It seems likely that this is due to contributions to the exchange reaction kinetics from hydrogen-bonding interactions between the incoming diol and the coordinated diolate that are weakened in pyridine (cf. rapid intramolecular exchange of coordinated phenoxide and intermolecular hydrogen bonded phenol in $L_2Pd(Me)(OPh)$·HOPh complexes[28,31]). When the incoming diol is already intramolecularly hydrogen bonded, as in the (dppp)Pt(alditolate) complexes,[1] complexation isomer equilibration is rapid (minutes or less) in both dichloromethane and pyridine, consistent with our finding above that the intramolecular hydrogen bond should still be present in pyridine in these complexes.

Implications for Metal−Carbohydrate Chemistry. Regioselective complexation of alditols to $(dppp)Pt^{II}$ depends on the interplay of several factors. Normal terminal vs internal ligand complexation preferences, resulting from steric and electronic substitutent effects, are compounded in these complexes by axial vs equatorial substitution in the resulting dioxaplatinacyclopentane ring system and by hydrogen-bonding interactions of the "spectator" hydroxyls. In the absence of these latter two effects, we would expect terminal alditol complexation to be favored over internal complexation (based on the smaller steric hindrance posed by a single substituent in the terminal isomer and by the slightly greater acidity expected for a primary terminal CH_2-OH group over a secondary internal CHROH group), but independent experimental verification of this is difficult. Ligand steric and electronic effects can, however, be demonstrated to be a factor in axial vs equatorial substitution. On the basis of $^{195}Pt-O-C-^{13}C$ Karplus-type coupling constant patterns in (dppp)Pt(alkanediolate) complexes, methyl metallacycle substituents favor an equatorial disposition over an axial one by ∼0.15 kcal/mol per methyl group.[1] The bulkier phenyl and *tert*-butyl groups show much stronger equatorial preferences (based on $J_{PtC} = 40$ Hz in both compounds compared to 55 Hz for equatorial carbons and ∼−5 Hz for axial carbons (cf. Experi-

(55) Olovsson, I.; Jönsson, P.-G. In *The Hydrogen Bond. Recent Developments in Theory and Experiments. II. Structure and Spectrospcopy*; Schuster, P., Zundel, G., Sandorfy, C., Eds.; North-Holland: New York, 1976; Vol. II, pp 393−456.

(56) Perkampus, H. H.; Miligy, F.; Kerim, A. *Spectrochim. Acta* **1968**, *24A*, 2071−2079.

(57) Kulevsky, N.; Lewis, L. *J. Phys. Chem.* **1972**, *76*, 3502−3503.

(58) Prabhumirashi, L. S. *J. Chem. Soc., Faraday Trans. 2* **1978**, *74*, 1567−1572 and prior work cited therein.

(59) IR studies have also been reported for α,ω-diols (Busfield, W. K.; Ennis, M. P.; McEwen, I. J. *Spectrochim. Acta* **1973**, *29A*, 1259−1264) and 4-(hydroxymethyl)-1,3-dioxolanes (Aksnes, G.; Albriktsen, P. *Acta Chem. Scand.* **1966**, *20*, 1330−1334), but these suffer from flawed experimental protocols such as assuming equal extinction coefficients for free and hydrogen bonded hydroxyls or temperature independence of the extinction coefficients.

(60) Calculated from data in ref 57.

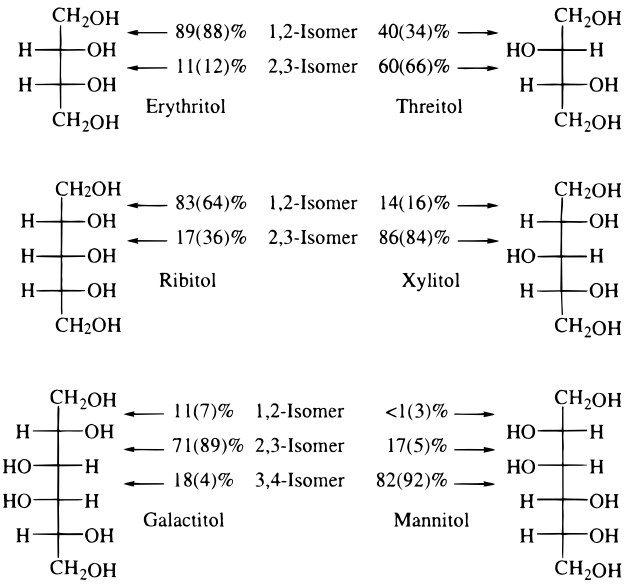

Figure 5. Alditol structures and observed equilibrium complexation regioselectivities for derived (dppp)Pt(alditolate) complexes in dichloromethane (from ref 1) and, in parentheses, pyridine (this work).

mental Section and ref 1)). Preliminary results suggested that there might also be an electronic component to axial−equatorial preferences since the methoxymethyl substituent in the (dppp)-Pt(3-methoxy-1,2-propanediolate) complex appeared to favor an *axial* disposition over an equatorial one by ∼0.5 kcal/mol.[1] This conclusion assumed that the Karplus equation for this complex is not significantly influenced by the electronegative substituent present, a potential problem.[61,62] The validity of this assumption for the Pt alditolate complexes, however, has been confirmed in the current study by examining the ^{13}C NMR of the (dppp)Pt^{II} complex of methyl 4,6-*O*-benzylidene-α-glucopyranoside. The two $^{195}Pt-O-C-^{13}C_\alpha$ coupling constants in this conformationally locked system are both 56 Hz, essentially identical to that of 55 Hz found for our previous Karplus calibration complex (dppp)Pt(*trans*-cyclohexane-1,2-diolate).[1] This apparent electronic preference of oxymethyl substitutents for axial configurations may be augmented when there are spectator hydroxyl groups present, since axial configurations permit hydrogen bonding of the substituent hydroxyl(s) to the farther Pt-bound oxygen. This leads to larger hydrogen bond ring sizes, more linear O−H···O bonds, and hence stronger hydrogen bonds. These preferences for axial substitution are undoubtedly responsible for the observed predominance in alditolate complexes for complexation of *threo* diol units over *erythro* diol units (cf. Figure 5),[1] the former allowing access to diaxial configurations while the latter necessarily involving mixed ax, eq configurations.

The intramolecular hydrogen bond free energy strengths of ∼2−2.5 kcal/mol found here for the (dppp)Pt(triolate) complexes probably represent a lower limit for those present in the (dppp)Pt(alditolate) complexes. First, the alditolate hydroxyl groups should be slightly more acidic than that of the isolated 4-hydroxyl group in the 1,2,4-butanetriol model employed here. Second, when a polyhydroxy side chain is present, as in the 3,4-mannitolate complex (Figure 1), the first hydrogen bond that is formed carries the entropic penalty of rotational "locking" of the side chain. Any additional hydrogen bonds formed by the other hydroxyls in the side chain then carry a smaller entropic penalty and may in fact lead to an increase in entropy due to the formation of new vibrational modes.[4] It seems likely that this factor, along with the larger hydrogen-bonding ring size accessible, contributes to the observed preference for regioselectivities favoring dihydroxyethyl substitution over hydroxymethyl substitution.[1]

On balance, while individual hydrogen bonds are undoubtedly stronger than the axial−equatorial substitution preferences, each alditol complexation isomer typically involves some combination of hydrogen bonds. It is therefore the much smaller *differences* in total hydrogen bond energies between the isomers compared to the ax/eq energy differences that actually determine the regioselectivities. Furthermore, many different equilibrium permutations of hydrogen bond ring sizes may be accessible in these systems, determined interactively with axial vs equatorial and terminal vs internal substitution patterns. As a result, while *a priori* prediction and rigorous *post facto* quantitiative analysis of regioselectivities are difficult, experimental determination of these trade-offs is readily achieved in the bis(phosphine)-platinum(II) system (Figure 5).

The present work also offers some insights into the solvent effects on the (dppp)Pt(alditolate) complexation regioselectivities. As seen in the triol model studies, switching from dichloromethane to pyridine reduces the apparent strengths of both "five"- and "six"-membered hydrogen bond ring systems by a comparable amount, namely, the 1.6 kcal/mol free energy of the pyridine−hydroxyl hydrogen bond. As long as the different complexation isomers for an alditol have the same total number of intramolecular hydrogen bonds, each isomer will have its energy changed by essentially the same amount on switching solvents. This leads to the otherwise somewhat surprising observed result that the isomer ratios are generally independent of solvent (cf. Figure 5). Some regioisomers, however, have a hydroxyl group that is geometrically precluded from participating in intramolecular hydrogen bonding. On switching from dichloromethane to pyridine solution, such a hydroxyl will form a *new*, intermolecular hydrogen bond to the pyridine, lowering the energy of this isomer relative to other isomers in which all the hydroxyls are/were intramolecularly hydrogen bonded. This would explain the increase in certain isomers on going from dichloromethane to pyridine solution, e.g., 3,4-mannitolate (cf. Figure 1), 2,3-galactitolate, and 2,3-ribitolate, which from X-ray structures[1,3] and/or molecular models each have isolated hydroxyls not involved in intramolecular hydrogen bonds.

Experimental Section

General Information. All operations were carried out under argon using glovebox and Schlenk techniques unless otherwise noted. Phenol (Aldrich, 99.8%), triphenylphosphine oxide (Aldrich, 98%), 3-methoxypropanediol (Aldrich, 98%), 1,2,4-butanetriol (Aldrich, 96% for synthetic preparations), (*S*)-(−)-1,2,4-butanetriol (Aldrich, 98% for equilibrium studies), glycerol (Mallinkrodt, 99.5%), and methyl (+)-4,6-*O*-benzylidene-α-D-glucopyranoside (Aldrich) were used as received. Phenyl-1,2-ethanediol ($PedH_2$, Aldrich) was purified by extraction of yellow impurities with a minimal volume of ether and then sublimation of the residue at 60 °C under vacuum. Dichloromethane-d_2 (Cambridge Isotope Laboratories) was distilled from P_2O_5. Butane-1,2,4-triol was treated with acetone to give 1,2-*O*-isopropylidenebutane-1,2,4-triol[63] which was in turn converted to 4-methoxybutane-1,2-diol (97% purity) by treatment with sodium hydride and methyl iodide.[64] Platinum complexes were prepared as described previously.[1] ^1H and ^{31}P NMR spectra (Bruker AM-300) of the (dppp)-Pt(Ped) used for the phenol titration showed that it contained 0.88 equiv of CH_2Cl_2 and ≤1% (dppp)$PtCl_2$. Proton NMR chemical shifts were referenced to the residual $CHDCl_2$ center peak at 5.32 ppm. NMR

(61) Haasnoot, C. A. G.; de Leeuw, F. A. A. M.; Altona, C. *Tetrahedron* **1980**, *36*, 2783−2792.
(62) Kalinowski, H.-O.; Berger, S.; Braun, S. *Carbon-13 NMR Spectroscopy*; Wiley: New York, 1988.
(63) Hayashi, H.; Nakanishi, K.; Brandon, C.; Marmur, J. *J. Am. Chem. Soc.* **1973**, *95*, 8749−8757.
(64) Kelly, J. W.; Evans, S. A. J. *J. Am. Chem. Soc.* **1986**, *108*, 7681−7685.

probe temperatures were calibrated with methanol as described in the literature.[65] Unless otherwise noted, weighings were accurate to ±0.2 mg and volumetric flask measurements to ±1%, and syringe measurements to ±1−2%. The density of CH_2Cl_2 at 295 K was taken to be 1.325 g/mL, that of CD_2Cl_2 to be 1.362 g/mL.[66] The latter's temperature dependence was assumed to have the same percentage variation as that of CH_2Cl_2, which is given by the formula (molar density d for T in K):[67]

$$d = 1.3897/(0.25678^{(1+(1-T/510)^{0.2902})}$$

Synthesis of (dppp)Pt(4-methoxy-1,2-butanediolate). The complex was prepared analogously to other (dppp)Pt(diolate) complexes;[1] thus, (dppp)Pt(CO_3) (179 mg, 269 μmol) and 4-methoxy-1,2-butanediol (50.9 mg, 420 μmol, 1.56 equiv) were dissolved in CH_2Cl_2 (15 mL) in a 25 mL Schlenk flask. The solution was stirred for 2 h under argon, during which time the solution was bubbled with argon for 1 min every 15 min. At this time, a ^{31}P NMR spectrum showed that the reaction was only 65% complete, so an additional quantity of 4-methoxy-1,2-butanediol (14.2 mg, 117 μmol, 2.0 equiv total) was added. After stirring an additional 2.5 h with periodic bubbling with argon, another NMR spectrum indicated that the reaction was 97% complete. The reaction mixture was allowed to stand for another 30 min and then the volume of the reaction mixture was reduced. The solution was transferred to a diffusion tube, concentrated to a total volume of 3 mL, and then layered with ether (25 mL). Diffusion over 48 h yielded white crystals of (dppp)Pt(4-methoxy-1,2-butanediolate) which were washed with cold ether (4 × 2 mL) and vacuum dried. The supernatant was evaporated; the residue was redissolved in a minimum of CH_2Cl_2 (2 mL) and layered with ether again (20 mL). Diffusion over 72 h at room temperature yielded a second crop. Total yield was 109 mg, 56%, of spectroscopically pure material. ^{31}P NMR (CD_2Cl_2): δ −8.48 (d with ^{195}Pt satellites, J_{PP} = 32 Hz, J_{PtP} = 3131 Hz), −8.83 (d with ^{195}Pt satellites, J_{PP} = 32 Hz, J_{PtP} = 3141 Hz). ^{1}H NMR (CD_2Cl_2): δ 7.8 (m, 8 H), 7.3 (m, 12 H), 3.75 (m, 1 H, PtOC*H*CH_2CH_2OMe), 3.67 (ddd, J_{HH} = 9.1, 4.0 Hz, J_{PH} = 4.0 Hz, 1 H, PtOCH_AH_B), 3.40 (ddd, J_{HH} = 9.1, 6.0 Hz, J_{PH} = 3.0 Hz, 1 H, PtOCH_AH_B), 3.28 (t, J_{HH} = 7.4 Hz, 2 H, CH_2CH_2OMe), 3.19 (s, 3 H, OCH_3), 2.4 (m, 4 H, PCH_2), 1.95 (m, 2 H, PCH_2CH_2), 1.74 (d of t, J_{HH} = 5.8, 7.4 Hz, 2 H, CH_2-OMe). ^{13}C{^{1}H} NMR (CD_2Cl_2): δ 133.8 (m), 131.0 (m), 128.7 (m), 81.8 (dd, J_{PC} = 4.7, 2.4 Hz, PtOC_A), 80.7 (dd, J_{PC} = 4.5, 2.6 Hz, PtOC_B), 72.1 (s, CH_2OMe), 58.5 (s, OCH_3), 35.6 (br s, with Pt satellites, J_{PtC} = 22 Hz, CH_2CH_2OMe), 26.0 (dd, J_{PC} = 34.5, 7.7 Hz, P_ACH_2), 25.7 (dd, J_{PC} = 34.0, 7.3 Hz, P_BCH_2), 20.3 (s, with Pt satellites, J_{PtC} = 20 Hz).

Synthesis of (dppp)Pt(3,3-dimethyl-1,2-butanediolate). This was prepared analogously to the ethanediolate complex,[1] yield 45%. ^{31}P{^{1}H} NMR (CD_2Cl_2): δ −8.5 (d with Pt satellites, J_{PP} = 31.4 Hz, J_{PtP} = 3096 Hz), −10.6 (d with Pt satellites, J_{PP} = 31.4 Hz, J_{PtP} = 3127 Hz). ^{1}H NMR (CD_2Cl_2) (second-order analysis utilizing the Bruker Panic program): δ 7.85 (m, 6 H, Ph), 7.81 (m, 2 H, Ph), 7.38 (m, 12 H, Ph), 3.68 (m, J_{HH} = 10.1, (−)9.1 Hz, J_{PH} ≈ 0 Hz, 1 H, OCH_BH_C), 3.59 (m, J_{HH} = 10.1, 3.8 Hz, J_{PH} ≈ 0 Hz, 1 H, OCH_A-*t*-Bu), 3.52 (m, J_{HH} = (−)9.1, 3.8 Hz, J_{PH} = 8.6, (−)2.2 Hz, 1 H, OCH_BH_C), 2.40 (br m, 4 H, PCH_2), 1.95 (br m, 2 H, PCH_2CH_2), 0.82 (s, 9 H, CH_3). ^{13}C{^{1}H} NMR (CD_2Cl_2): δ 134.0 (d, J_{PC} = 10.1 Hz, J_{PtC} = 20 Hz, *ortho* C), 133.9 (d, J_{PC} = 10.7 Hz, J_{PtC} obscured, *ortho* C), 133.8 (d, J_{PC} = 10.1 Hz, J_{PtC} obscured, *ortho* C), 133.4 (d, J_{PC} = 10.8 Hz, J_{PtC} = 20 Hz, *ortho* C), 131.8 (d, J_{PC} = 58 Hz, *ipso* C), 131.7 (d, J_{PC} = 58 Hz, *ipso* C), 131.6 (d, J_{PC} = 58 Hz, *ipso* C), 131.3 (d, J_{PC} = 58 Hz, *ipso* C), 130.9 (d, J_{PC} = 2.8 Hz, *para* C), 130.9 (d, J_{PC} = 2.4 Hz, *para* C), 130.8 (d, J_{PC} = 2.9 Hz, *para* C), 130.7 (d, J_{PC} = 2.8 Hz, *para* C), 128.7 (d, J_{PC} = 10.6 Hz, *meta* C), 128.6 (d, J_{PC} = 10.6 Hz, *meta* C), 128.4 (d, J_{PC} = 10.5 Hz, *meta* C), 128.3 (d, J_{PC} = 10.7 Hz, *meta C*), 92.8 (dd, J_{PC} = 5.2, 3.4 Hz, OCH), 76.1 (dd, J_{PC} = 5.0, 3.9 Hz, OCH_2), 34.2 (d, J_{PC} = 3 Hz, J_{PtC} = 40 Hz, $C(CH_3)_3$), 27.6 (s, CH_3), 26.1 (dd, J_{PC} = 38.3, 3.8 Hz, J_{PtC} = 27 Hz, PC_AH_2), 24.9 (dd, J_{PC} = 38.3, 3.6 Hz, J_{PtC} = 27 Hz, PC_BH_2), 20.4 (s, J_{PtC} = 21 Hz, PCH_2CH_2).

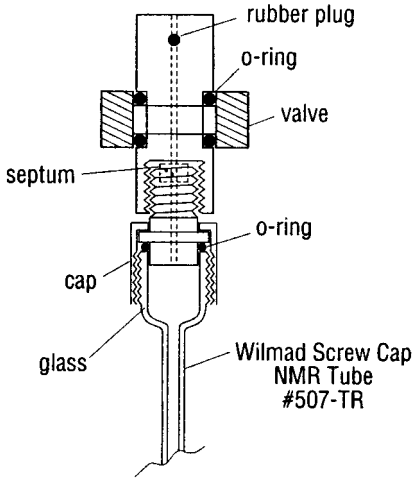

Figure 6. Design of home-built valved NMR tube cap.

Synthesis of (dppp)Pt(methyl 2,3-*O,O′*-diolato-4,6-*O*-benzylidene-α-D-glucopyranoside). (dppp)Pt(CO_3) (258.6 mg, 387 μmol) and methyl 4,6-*O*-benzylidene-α-D-glucopyranoside (234.8 mg, 832 μmol, 2.14 equiv) were dissolved in CH_2Cl_2 (20 mL) in a 100 mL Schlenk flask. The flask was partially evacuated and refilled with argon (about sets of three cycles repeated once per hour) over a 8 h period and then the solution allowed to stir overnight, at which time a ^{31}P NMR showed 97% conversion to product. The solution was concentrated to 2−3 mL and layered with ether (∼15 mL). The resulting white precipitate was isolated by centrifugation, washed with ether (2 × 20 mL), and dried under vacuum to give the desired product (310 mg, 90%), spectroscopically pure except for a trace of ether (2 mol %). ^{31}P NMR (CD_2Cl_2): δ −9.73 (d with ^{195}Pt satellites, J_{PtP} = 3224 Hz, J_{PP} = 32 Hz), −10.11 (d with ^{195}Pt satellites, J_{PtP} = 3170 Hz, J_{PP} = 32 Hz). ^{1}H NMR (CD_2Cl_2): δ 7.9 (m, 8 H), 7.35 (m, 17 H), 5.47 (s, C*H*Ph), 4.77 (d, J_{HH} = 3.4 Hz, C*H*OMe), 4.23 (dd, J_{HH} = 9.7, 4.4 Hz, CH_AH_B), 4.04 (∼t, J_{HH} ≈ 9.1, PtOC*H*CHCHOMe), 3.72 (∼t, J_{HH} ≈ 10 Hz, H_AH_B), 3.72 (dd, J_{HH} = 9.5, 3.4 Hz, PtOC*H*CHOMe), 3.60 (∼ddd, J_{HH} ≈ 10, 9, 4.4 Hz, C*H*CH_2), 3.50 (∼t, J_{HH} ≈ 9 Hz, C*H*OCHPh), 3.39 (s, OCH_3), 2.4 (br m, 4 H, PCH_2), 1.95 (m, 2 H, PCH_2CH_2). ^{13}C{^{1}H} NMR (CD_2Cl_2): δ 139.1 (s), 134 (m), 131.2 (m), 128.7 (m), 128.3 (s), 126.8 (s), 104.2 (d, J_{PC} = 4.9 Hz, with Pt satellites, J_{PtC} = 56 Hz, PtOCH*C*HOMe), 101.2 (s, *C*HPh), 86.3 (dd, J_{PC} = 4.2, 2.7 Hz, PtO*C*), 85.7 (d, J_{PC} = 2.9 Hz, with Pt satellites, J_{PtC} = 56 Hz, PtOCH*C*HOCHPh), 82.4 (dd, J_{PC} = 4.0, 2.9 Hz, PtO*C*), 69.6 (s, [^{13}C: t, J_{CH} = 146 Hz], $CHCH_2$), 64.2 (s, [^{13}C: d, J_{CH} = 146 Hz], CH_2), 55.6 (s, [^{13}C: q, J_{CH} = 140 Hz], OCH_3), 25.9 (dd, J_{PC} = 36.2, 7.3 Hz, P_ACH_2), 25.8 (dd, J_{PC} = 35.8, 7.5 Hz, P_BCH_2), 20.2 (s, with Pt satellites, J_{PtC} = 21 Hz, PCH_2CH_2).

NMR of (dppp)Pt(Ped). A ^{13}C{^{1}H} NMR of (dppp)Pt(Ped), obtained at higher concentrations than that used in ref 1, permitted J_{PtC}, 40 Hz, for the phenyl-1,2-ethanediolate *ipso* carbon to be determined.

Determination of Effective Density of $OPPh_3$ in CH_2Cl_2. Triphenylphosphine oxide (178.1 mg) was dissolved in CH_2Cl_2 (1.1354 g, calculated to be 0.857 mL), which gave exactly 1.00 mL of total solution in a screw-capped volumetric flask. From this, the effective volume of the $OPPh_3$ was 0.14 mL, giving an effective density of 1.24(9) g/mL.

Titrations of Phenol with $OPPh_3$. In a typical titration, a stock solution of phenol (19.3 mg, 205 μmol in CD_2Cl_2 (1.1072 g)) was prepared in a screw-capped vial equipped with a Mininert Microflex valve (Kontes), which, based on a total volume of 0.829 mL ((1.1072 + 0.0193)/1.362, assuming within experimental error that the effective density of PhOH is equal to that of CD_2Cl_2 at this low concentration), corresponded to a phenol concentration of 247 mM. A 10.0 μL aliquot of this solution was added to CD_2Cl_2 (0.5827 g, 0.4278 mL) in a screw-capped NMR tube equipped with a special home-built valve modeled after the Mininert Microflex valve (Figure 6, see Supporting Information for design details) to give a 5.7(1) mM solution of phenol. A typical

(65) Van Geet, A. L. *Anal. Chem.* **1970**, *42*, 679−680.
(66) *Aldrich Catalog Handbook of Fine Chemicals*; Aldrich Chemical Co., Milwaukee, WI, 1994−1995.
(67) From the Design Institute for Physical Property Data (DIPPR) file, American Institute of Chemical Engineers (AIChe) accessed via the Scientific and Technical Information Network (STN).

stock solution of triphenylphosphine oxide (118.4 mg, 425.5 μmol in CD_2Cl_2 (1.0108 g)) was prepared in a second screw-capped vial equipped with a Mininert valve, which, based on a total volume of 0.837 mL (1.0108/1.362 + 0.1184/1.24), corresponded to a phosphine oxide concentration of 508(10) mM. Sequential aliquots (15−20 of 10−100 μL each) of the phosphine oxide stock solution were then added to the NMR tube using Hamilton series 1700 gas-tight syringes with 26S gauge, point style no. 5 needles (the syringe being washed between aliquots with CH_2Cl_2 and vacuum dried at 55 °C to prevent introduction of adventitious water) and the tube was thoroughly mixed. To confirm the accuracy of the multiple-aliquot protocol and to check for loss of solvent due to evaporation at elevated temperatures, the total volume of the solution was verified after addition of each aliquot by comparison of the calculated volume with that determined by measuring the height of the solution and applying a published height-to-volume conversion formula.[68] Phenol-to-phosphine oxide ratios were also checked by NMR integration. After addition of the final aliquot of phosphine oxide, the concentration of phenol was ∼2.5 mM and that of phosphine oxide ∼0.3 M for a typical titration. Proton NMR spectra (0.25 Hz digital resolution) were recorded before adding any phosphine oxide and after addition of each aliquot, allowing at least 7 min for temperature equilibration in the probe (298.3(8) K). Comparable experiments were conducted with fresh stock solutions at 264 (two independent runs), 274 (one run), 284 (one run), 298 (two runs), and 304 K (two runs), the concentration data being corrected for temperature effects on solution volumes. Tables of the resulting titration data giving [PhOH], [$OPPh_3$], and ^{1}H NMR chemical shift of the phenol OH proton are included in the Supporting Information. The OH chemical shift typically changed from δ 4.8 to ∼10. The experimental titration data covered >90−95% of the calculated total phenol chemical shift range.

Titrations of Phenol with (dppp)Pt(Ped). These titrations were conducted analogously to those for $OPPh_3$ except as noted here. A typical stock solution of (dppp)Pt(Ped)·0.88CH_2Cl_2 (19.3 mg, 23.6 μmol in CD_2Cl_2 (1.1673 g)) was prepared in a screw-capped vial equipped with a Mininert valve, which, based on a total volume of 0.871 mL ((1.1673 + 0.0193)/1.362, assuming within experimental error that the effective density of (dppp)Pt(Ped) is equal to that of CD_2Cl_2 at this low concentration), corresponded to a Pt concentration of 27.1(5) mM. The number and size of the Pt aliquots (10−15 of 10−250 μL each) were chosen to effectively sample significant portions of the calculated total phenol chemical shift range, i.e., from 0 to 83−96% for low-temperature runs and 0 to 72−83% for high-temperature runs. After addition of the final aliquot of Pt, the concentration of phenol was typically ∼2 mM and that of Pt ∼15 mM. Proton NMR spectra taken with adequate relaxation delays at various points showed reasonable agreement between the observed and calculated stoichiometries as well as a water level below 1 mol %. Following each titration, ^{31}P NMR check spectra showed the presence of less than 1.5% (dppp)$PtCl_2$ and no discernable (dppp)Pt$(OPh)_2$. Duplicate runs were carried out at each of five temperatures (267, 280, 298, 307, and 321 K, calibrated with methanol at the start and end of each titration) using fresh Pt stock solutions for each run and fresh phenol stock solutions at each temperature, the concentration data being adjusted for the temperature effect on solution volumes. Tables of the resulting titration data giving [PhOH], [Pt], and ^{1}H NMR chemical shift of the phenol OH proton are included in the Supporting Information.

Decomposition Reactions of (dppp)Pt(diolates) in CD_2Cl_2. A solution of (dppp)Pt(1,2-propanediolate) (10.9 mg, 16.0 μmol) in CD_2Cl_2 (0.55 mL) was allowed to stand in the drybox for 48 days. A ^{31}P NMR spectrum taken at that time showed the phosphorus-containing components to be a mixture of (dppp)$PtCl_2$ (67%), (dppp)Pt(1,2-propanediolate) (32%), and (dppp)Pt(CO_3) (<1%). A ^{1}H NMR spectrum of the solution exhibited peaks consistent with formation of 4-methyl-1,3-dioxolane-2-d_2: δ 4.09 (approximate sextet, $J \approx 6.3$ Hz, 1H, OC*H*), 3.95 (dd, $J = 7.6$, 6.4 Hz, 1H, OCH_AH_B), 3.31 (t, $J = 7.3$ Hz, 1H, OCH_AH_B), 1.25 (d, $J = 6.1$ Hz, 3H, CH_3). The GC−MS fragmentation pattern of the major volatile species was also consistent with 4-methyl-1,3-dioxolane-2-d_2 based on comparison with a library spectrum of all-*protio* 4-methyl-1,3-dioxolane. Similar behavior was observed for the diolate complexes employed in the present study, conversion to (dppp)$PtCl_2$ at 40 °C in dichloromethane solution occurring at rates of ∼0.1%/h for the triolate complexes and 0.3%/h for the methoxydiolate complexes.

Diol−Diolate Exchange Reactions. General Information. Stock solutions containing ∼1:1 mixtures of the appropriate diol/triol and (dppp)Pt(diolate/triolate) were prepared in the chosen solvent as described below, taking into account the limited solubilities of glycerol and 1,2,4-butanetriol in dichloromethane (determined to be 6.5 and 11.5 mM, respectively, by ^{1}H NMR integration of saturated solutions vs an internal standard; 3-methoxy-1,2-propanediol had a solubility of ≥0.28 M in dichloromethane). Aliquots of the diol−diolate stock solutions were transferred to NMR tubes equipped with a J. Young valve, thermostated at 40 °C, and monitored by ^{31}P NMR until the reaction reached equilibrium (days in pyridine, hours in dichloromethane). When feasible, ^{1}H NMR spectra were used to verify the relative diol to diolate concentrations in the stock solutions. Final ^{31}P spectra for determination of equilibrium constants were acquired with 0.19 Hz digital resolution, a 1−2 Hz line-broadening (exponential smoothing) function, and sufficient scans (∼1200−2500) to insure good signal-to-noise ratios. Test spectra collected with inverse-gated decoupling gave integration ratios indistinguishable from those collected with standard CPD decoupling, a 60° pulse width, and a 5.4 s acquisition time, indicating that differences in NOE and relaxation times (∼6 s) between the complexes are negligible. For each spectrum, three separate integrations were performed, starting from the raw FID each time. Using only the main lines due to non-^{195}Pt-containing species, two integrals were determined for each spectrum, one for half of the AB quartet due to the triolate complex, the other for the second half of the AB quartet of the triolate complex plus the full AB quartet due to the methoxydiolate complex. Any other species present (i.e., (dppp)$PtCl_2$) were also integrated. The sum of all integrals was set to 100%. With these precautions, integrations were reproducible to ±1−2%. Using these integrals, the initial diol and diolate complex concentrations, and reaction stoichiometries, the final concentrations of all four species contributing to the diol−diolate equilbrium constant expression were calculated. Reactions were considered to have reached equilibrium when three successive spectra gave the same computed equilibrium constants within experimental error.

A. (dppp)Pt(3-methoxy-1,2-propanediolate) + Glycerol in Pyridine-d_5. Stock solutions of (dppp)Pt(3-methoxy-1,2-propanediolate) (10.6 mg, 14.9 μmol) and glycerol (6.2 mg, 67 μmol) in pyridine-d_5 were prepared in separate 1.00 mL volumetric flasks. Aliquots of the (dppp)Pt(3-methoxy-1,2-propanediol) (270 μL) and glycerol (60 μL) stock solutions were added to a third 1.00 mL volumetric flask and diluted to the mark with pyridine-d_5 to give final concentrations of (dppp)Pt(3-methoxy-1,2-propanediol) of 4.02 mM and of glycerol of 4.02 mM. Solution compositions determined by ^{31}P NMR at 14, 121.5, 185.5, 277.5, and 353.5 h were (% Pt diolate:% Pt triolate) 77.3:22.7, 37.5:62.5, 37.9:62.1, 38.6:61.4, and 37.5:62.5, respectively, giving K_{rel} values (eq 5) of 2.73, 2.66, 2.51, and 2.76 for the last four "equilibrium" data points for an average value of 2.7 ± 0.1. Calculation of K_{rel} is illustrated for the last data point: [(dppp)Pt(3-methoxy-1,2-propanediolate)] = 0.375 × 4.02 = 1.51 mM, [(dppp)Pt(glycerolate)] = [3-methoxy-1,2-propanediol] = 0.625 × 4.02 = 2.51mM, and [glycerol] = 4.02−2.51 = 1.51 mM, giving $K_{rel} = (2.51)^2/(1.51)(1.51) = 2.76$.

B. (dppp)Pt(glycerolate) + 3-Methoxy-1,2-propanediol in Pyridine-d_5. Stock solutions of (dppp)Pt(glycerolate)·0.05CH_2Cl_2 (14.2 mg, 20.2 μmol) and 3-methoxy-1,2-propanediol (12.4 mg, 117 μmol) in pyridine-d_5 were prepared in 1.00 and 2.00 mL volumetric flasks, respectively. Aliquots of the (dppp)Pt(glycerolate) (200 μL) and 3-methoxy-1,2-propanediol (70 μL) stock solutions were added to another 1.00 mL volumetric flask and diluted to the mark with pyridine-d_5 to give final concentrations of (dppp)Pt(glycerolate) of 4.04 mM and of 3-methoxy-1,2-propanediol of 4.09 mM. Solution compositions determined by ^{31}P NMR for five data points from 200 to 400 h were (% Pt diolate:% Pt triolate) 37.9:62.1, 37.3:62.7, 38.3:61.7, 37.8:62.2, and 38.2:61.8, giving K_{rel} values of 2.74, 2.88, 2.65, 2.76, and 2.66, for an average value of 2.7 ± 0.1.

C. (dppp)Pt(3-methoxy-1,2-propanediolate) + Glycerol in CH_2Cl_2. Stock solutions of (dppp)Pt(3-methoxy-1,2-propanediolate)·0.5CH_2Cl_2 (114.8 mg, 19.6 μmol) and glycerol (11.8 mg, 128 μmol) in CH_2Cl_2 were prepared in 1.00 and 25.0 mL volumetric flasks, respectively. Aliquots of the (dppp)Pt(3-methoxy-1,2-propanediol) (200 μL) and

(68) Bryndza, H. E.; Calabrese, J. C.; Marsi, M.; Roe, D. C.; Tam, W.; Bercaw, J. E. *J. Am. Chem. Soc.* **1986**, *108*, 4805−4813.

glycerol (800 μL) stock solutions were added directly to the NMR tube to give final concentrations of (dppp)Pt(3-methoxy-1,2-propanediol) of 3.93 mM and of glycerol of 4.10 mM. Solution compositions determined by ^{31}P NMR for three data points from 300 to 500 min were (% Pt diolate:% Pt triolate:% Pt chloride) 14.7:84.6:0.7, 13.8:85.3:0.9, and 13.8:85.2:1.0, giving K_{rel} values of 24.2, 27.3, and 26.8 (assuming all (dppp)$PtCl_2$ resulting from (dppp)Pt(3-methoxy-1,2-propanediolate)) and 25.3, 28.9, and 28.6 (assuming all (dppp)$PtCl_2$ resulting from (dppp)Pt(glycerolate)). The average of the last two "equilibrium" data points by each method is 27.1 and 28.8, respectively.

D. (dppp)Pt(glycerolate) + 3-Methoxy-1,2-propanediol in CD_2Cl_2. Stock solutions of (dppp)Pt(glycerolate)·0.05CH_2Cl_2 (13.9 mg, 19.8 μmol) and 3-methoxy-1,2-propanediol (14.5 mg, 137 μmol) in CD_2Cl_2 were prepared in separate 1.00 volumetric flasks. Aliquots of the (dppp)Pt(glycerolate) (200 μL) and 3-methoxy-1,2-propanediol (30 μL) stock solutions were added to a third 1.00 mL volumetric flask and diluted to the mark with CD_2Cl_2 to give final concentrations of (dppp)Pt(glycerolate) of 3.96 mM and of 3-methoxy-1,2-propanediol of 4.10 mM. Solution compositions determined by ^{31}P NMR for three data points from 500 to 1100 min were (% Pt diolate:% Pt triolate:% Pt chloride) 16.8:82.6:0.6, 16.5:81.7:1.8, 16.8:81.3:1.9, giving K_{rel} values of 25.2, 25.6, and 24.4 (assuming all (dppp)$PtCl_2$ resulting from (dppp)Pt(3-methoxy-1,2-propanediolate)) and 26.4, 29.4, and 28.1 (assuming all (dppp)$PtCl_2$ resulting from (dppp)Pt(glycerolate)). The average value by each method is 25.1 and 28.0, respectively.

E. (dppp)Pt(4-methoxy-1,2-butanediolate) + 1,2,4-Butanetriol in Pyridine-d_5. Stock solutions of (dppp)Pt(4-methoxy-1,2-butanediolate) (14.6 mg, 20.1 μmol) and 1,2,4-butanetriol (21.0 mg, 198 μmol) in pyridine-d_5 were prepared in separate 1.00 mL volumetric flasks. Aliquots of the (dppp)Pt(4-methoxy-1,2-butanediolate) (200 μL) and 1,2,4-butanetriol (20 μL) stock solutions were added to a third 1.00 mL volumetric flask and diluted to the mark with pyridine-d_5 to give final concentrations of (dppp)Pt(4-methoxy-1,2-butanediolate) of 4.02 mM and of 1,2,4-butanetriol of 3.96 mM. An aliquot of this solution was transferred to an NMR tube equipped with a J. Young valve, thermostated at 40 °C, and monitored by ^{31}P NMR over a period of days until the reaction reached equilibrium. Solution compositions determined by ^{31}P NMR for five data points from 220 to 340 h were (% Pt diolate:% Pt triolate) 34.5:65.5, 34.5:65.5 (inverse gated decoupled), 34.3:65.7, 34.6:65.4, and 34.4:65.6 (inverse gated decoupled), giving K_{rel} values (eq 6) of 3.77, 3.79, 3.85, 3.75, and 3.82, for an average value of 3.80 ± 0.04.

The NMR tube was then heated to 90 °C and monitored by ^{31}P NMR over a period of days (quenching the sample in an ice bath prior to each measurement). No detectable change in isomeric composition from the 40 °C values could be detected.

F. (dppp)Pt(1,2,4-butanetriolate) + 4-Methoxy-1,2-butanediol in Pyridine-d_5. Stock solutions of (dppp)Pt(1,2,4-butanetriolate) (15.0 mg, 20.6 μmol, corrected for the presence of 2.6% (dppp)Pt(CO_3)) and 4-methoxy-1,2-butanediol (15.6 mg, 125 μmol, corrected for the presence of 3% 1,2-*O*-isopropylidene-4-methoxy-1,2-butanediol) in pyridine-d_5 were prepared in separate 1.00 mL volumetric flasks. Aliquots of the (dppp)Pt(1,2,4-butanetriolate) (190 μL) and 4-methoxy-1,2-butanediol (35 μL) stock solutions were added to another 1.00 mL volumetric flask and diluted to the mark with pyridine-d_5 to give final concentrations of (dppp)Pt(1,2,4-butanetriolate) of 3.92 mM and of 4-methoxy-1,2-butanediol of 4.37 mM. Solution compositions determined by ^{31}P NMR for four data points from 90 to 180 h were (% Pt diolate:% Pt triolate) 36.4:63.6, 36.1:63.9, 36.6:63.3, and 36.5:63.5, giving K_{rel} values of 3.61, 3.70, 3.54, and 3.57, for an average value of 3.61 ± 0.07. A replicate experiment using independent stock solutions gave K_{rel} = 3.7 ± 0.1.

G. (dppp)Pt(4-methoxy-1,2-butanediolate) + 1,2,4-Butanetriol in CD_2Cl_2. Stock solutions of (dppp)Pt(4-methoxy-1,2-butanediolate) (7.3 mg, 10.1 μmol) and 1,2,4-butanetriol (10.5 mg, 99.0 μmol) in CH_2Cl_2 were prepared in 1.00 and 10.0 mL volumetric flasks, respectively. Aliquots of the (dppp)Pt(4-methoxy-1,2-butanediolate) (400 μL) and 1,2,4-butanetriol (400 μL) stock solutions were added to another 1.00 mL volumetric flask and diluted to the mark with CH_2Cl_2 to give final concentrations of (dppp)Pt(4-methoxy-1,2-butanediolate) of 4.02 mM and of 1,2,4-butanetriol of 3.96 mM. Solution compositions determined by ^{31}P NMR for three data points from 500 to 800 min were (% Pt diolate:% Pt triolate:% Pt chloride) 11.7:86.8:1.5, 12.2:86.2:1.5, and 11.7:86.5:1.8, giving K_{rel} values of 54.8, 48.7, and 53.2 (assuming all (dppp)$PtCl_2$ resulting from (dppp)Pt(4-methoxy-1,2-butanediolate)) and 64.0, 56.8, and 64.3 (assuming all (dppp)$PtCl_2$ resulting from (dppp)Pt(butanetriolate)). The average by each method is 52 and 62, respectively.

H. (dppp)Pt(1,2,4-Butanetriolate) + 4-Methoxy-1,2-butanediol in CD_2Cl_2. Stock solutions of (dppp)Pt(1,2,4-butanetriolate) (14.7 mg, 20.6 μmol) and 4-methoxy-1,2-butanediol (10.5 mg, 84.1 μmol, corrected for 3% impurity) in CD_2Cl_2 were prepared in 1.00 and 2.00 mL volumetric flasks, respectively. Aliquots of the (dppp)Pt(1,2,4-butanetriolate) (200 μL) and 4-methoxy-1,2-butanediol (100 μL) stock solutions were added to another 1.00 mL volumetric flask and diluted to the mark with CD_2Cl_2 to give final concentrations of (dppp)Pt(1,2,4-butanetriolate) of 4.13 mM and of 4-methoxy-1,2-butanediol of 4.21 mM. Solution compositions determined by ^{31}P NMR for four data points from 400 to 800 min were (% Pt diolate:% Pt triolate:% Pt chloride) 11.7:87.4:0.9, 12.4:86.5:1.1, 11.6:87.0:1.4, and 11.8:86.4:1.8, giving K_{rel} values of 57.3, 49.9, 58.0, and 54.6 (assuming all (dppp)$PtCl_2$ resulting from (dppp)Pt(4-methoxy-1,2-butanediolate)) and 62.7, 55.4, 67.2, and 65.6 (assuming all (dppp)$PtCl_2$ resulting from (dppp)Pt(butanetriolate)). The average by each method is 55 and 63, respectively.

Acknowledgment. The authors thank Nicole Brunkan (N.M.B.), George Gould, and Eric Voss for preliminary experiments related to these studies, Bruce Brunschwig for assistance in developing the data analysis routines, and Morris Bullock, Greg Hall, Marshall Newton, and Norman Sutin for helpful discussions. This research was carried out at Brookhaven National Laboratory under Contract DE-AC02-76CH00016 with the U.S. Department of Energy and supported by its Division of Chemical Sciences, Office of Basic Energy Research. Participation of Z.H.S. and N.M.B. in this work as Science and Engineering Research Students was supported by the U.S. Department of Energy's Office of University and Science Education Programs, Office of Energy Research.

Appendix

Data Analysis. (A) Monoadduct Formation. For the case in which only one hydrogen-bonding interaction is present, e.g., PhOH−$OPPh_3$, equations similar to 1 and 6 can be written as follows:

$$\delta_{obs} = \delta_o + \Delta\delta\ ([HBC]/[HBA_T]) \quad \text{(A1)}$$

$$K = [HBC]/[HBD][HBA] = [HBC]/(([HBD_T] - [HBC])([HBA_T] - [HBC])) \quad \text{(A2)}$$

where $[HBD_T]$ and $[HBA_T]$ are the total concentrations of all species involving the hydrogen bond donor and acceptor, respectively, [HBC] is the concentration of the hydrogen bond complex HBD···HBA, K is the hydrogen bond association constant, δ_o is the chemical shift of the free HBD, $\Delta\delta$ is the change in chemical shift of the HBD on full complexation, and δ_{obs} is the observed exchange-averaged chemical shift of the HBD. Rearranging and combining terms in eq A2 gives

$$[HBC]^2 - ([HBD_T] + [HBA_T] + 1/K)[HBC] + [HBD_T][HBA_T] = 0 \quad \text{(A3)}$$

Solving eq A3 for [HBC] gives

$$[HBC] = 1/2\{([HBD_T] + [HBA_T] + 1/K) \pm \{([HBD_T] + [HBA_T] + 1/K)^2 - 4[HBD_T][HBA_T]\}^{1/2}\} \quad \text{(A4)}$$

where the physically meaningful solution requires that 0 ≤

(69) Hodgman, C. D. In *Mathemetical Tables*, 10th ed.; Hodgman, C. D., Ed.; Chemical Rubber Publishing Co.: Cleveland, OH, 1954; p 295.

$[HBC] \leq [HBD_T]$. Substitution of the expression for [HBC] given by eq A4 into eq A1 gives an equation for δ_{obs} in terms of the three knowns $[HBA_T]$, $[HBD_T]$, and δ_o and the two unknowns K and $\Delta\delta$. This equation is suitable for nonlinear least-squares fitting by standard procedures to obtain values of K and $\Delta\delta$ from δ_o and a set of $[HBA_T]$, $[HBD_T]$, and δ_{obs} titration data.

(B) Diadduct Formation. For the case in which two hydrogen-bonding interactions are present, equations analogous to A1 and A2 can be written:

$$\delta_{obs} = \delta_o + \Delta\delta_1([HBC1]/[HBA_T]) + \Delta\delta_2([HBC2]/[HBA_T]) \quad (A5)$$

$$K_1 = [HBC1]/[HBD][HBA] \Rightarrow [HBC1] = K_1[HBD][HBA] \quad (A6)$$

$$K_2 = [HBC2]/[HBD][HBC1] \Rightarrow [HBC2] = K_2[HBD][HBC1] = K_1K_2[HBA][HBD]^2 \quad (A7)$$

$$[HBA_T] = [HBA] + [HBC1] + [HBC2] \quad (A8)$$

$$[HBD_T] = [HBD] + [HBC1] + 2[HBC2] \quad (A9)$$

Substituting values of [HBC1] and [HBC2] from eqs A6 and A7 into eqs A8 and A9 gives

$$[HBA_T] = [HBA] + K_1[HBD][HBA] + K_1K_2[HBA][HBD]^2 \quad (A10)$$

$$[HBD_T] = [HBD] + K_1[HBD][HBA] + 2K_1K_2[HBA][HBD]^2 \quad (A11)$$

Solving eq A10 for [HBA] gives

$$[HBA] = [HBA_T]/(1 + K_1[HBD] + K_1K_2[HBD]^2) \quad (A12)$$

Substituting the value of [HBA] from eq A12 into eq A11 gives

$$[HBD_T] = [HBD] + K_1[HBD][HBA_T]/(1 + K_1[HBA] + K_1K_2[HBA]^2) + 2K_1K_2[HBD]^2[HBA_T]/(1 + K_1[HBA] + K_1K_2[HBA]^2) \quad (A13)$$

Multiplying out eq A13 and collecting terms in [HBD] gives

$$[HBD]^3 + (1 + 2K_2[HBA_T] - K_2[HBD_T])[HBD]^2/K_2 + (1 + K_1[HBA_T] - K_1[HBD_T])[HBD]/K_1K_2 - [HBD_T]/K_1K_2 = 0 \quad (A14)$$

Equations A5 and A14 together define a set of equations suitable for nonlinear least-squares fitting to obtain values of $\Delta\delta_1$, $\Delta\delta_2$, K_1, and K_2 from δ_o and a set of $[HBA_T]$, $[HBD_T]$, and δ_{obs} titration data.

In practice, the fitting algorithm assumed trial values of K_1 and K_2 and solved eq A14 for [HBD], using a standard analytical solution for cubic equations,[69] for each pair of $[HBA_T]$ and-$[HBD_T]$ in the titration data set, again providing an if/then/else test to select the proper root such that $0 \leq [HBD] \leq HBD_T$. These values were then substituted into eq A12 to find [HBA] and then both substituted into eqs A6 and A7 to determine sets of [HBC1] and [HBC2] for substitution into eq A5. Equation A5 was then fit by linear least-squares to determine $\Delta\delta_1$ and $\Delta\delta_2$. The process was then repeated using new trial values of K_1 and K_2 until the least-squares errors between the calculated and observed sets of δ_{obs} data were minimized. For both the mono- and diadduct cases, the implementation of the algorithm was performed on a Macintosh computer using the MatLab environment,[36] employing their built-in Levenberg-Marquardt nonlinear least-squares fitting routine, for which custom subroutines to define the functional forms of eqs A1 and A3 or A5 and A14 were developed.

Monte Carlo Error Analyses. To estimate the errors in the fitting parameters, a method of random variations in the experimental data was used. For each set of titration data, the actual data were fit as described above to determine K_1, K_2, $\Delta\delta_1$, and $\Delta\delta_2$. A new, "virtual" data set was then obtained by randomly varying the values of $[HBD_T]$ and $[HBA_T]$ subject to the constraints described below. The new data set was then fit to obtain alternative values for the four fitting parameters. This process was repeated 50 times, discarding any data sets that gave physically meaningless (i.e., negative) values for the fitting parameters. The standard deviations of the fitting parameters in the 50 virtual data sets were taken as the standard deviations for the parameters obtained from fitting the actual experimental data. The random generation of virtual data sets was constrained such that the initial $[HBD_T]$ and $[HBA_T]$ concentrations in each virtual data set were distributed about their corresponding actual value with a standard deviation of $\pm 2\%$. This represents the systematic errors in stock solution preparations. The remaining HBA_T and HBD_T concentrations in the data sets were derived from these values by adjusting them to reflect the dilution and increased concentration, respectively, resulting from each added syringe aloquot, these aliquots being dispersed about the actual value by a standard deviation of $\pm 1\%$. These standard deviations were chosen to represent the estimated errors in the actual experimental protocol.

Supporting Information Available: Tables of experimental titration data, complete diagram of valved NMR cap (Figure S1), and a correlation plot of phenol H-bonding enthalpy−entropy relationship parameters *m* and *b* (Figure S2) (10 pages). See any current masthead page for ordering and Internet access instructions.

IC970860P